Imbalance of peptidoglycan biosynthesis alters the cell surface charge of *Listeria monocytogenes*

Lisa Maria Schulz[1], Patricia Rothe[3], Sven Halbedel[3], Angelika Gründling[2], Jeanine Rismondo[1,2*]

[1] Department of General Microbiology, Institute of Microbiology and Genetics, GZMB, Georg-August University Göttingen, Grisebachstr. 8, 37077 Göttingen, Germany

[2] Section of Molecular Microbiology and Medical Research Council Centre for Molecular Bacteriology and Infection, Imperial College London, London SW7 2AZ, United Kingdom

[3] FG11, Division of Enteropathogenic bacteria and *Legionella*, Robert Koch Institute, Burgstraße 37, 38855 Wernigerode, Germany

* Correspondence:
Dr. Jeanine Rismondo
jrismon@gwdg.de, Tel. +49-551-3923796

Abstract

The bacterial cell wall is composed of a thick layer of peptidoglycan and cell wall polymers, which are either embedded in the membrane or linked to the peptidoglycan backbone and referred to as lipoteichoic acid (LTA) and wall teichoic acid (WTA), respectively. Modifications of the peptidoglycan or WTA backbone can alter the susceptibility of the bacterial cell towards cationic antimicrobials and lysozyme. The human pathogen *Listeria monocytogenes* is intrinsically resistant towards lysozyme, mainly due to deacetylation and *O*-acetylation of the peptidoglycan backbone via PgdA and OatA. Recent studies identified additional factors, which contribute to the lysozyme resistance of this pathogen. One of these is the predicted ABC transporter, EslABC. An *eslB* mutant is hyper-sensitive towards lysozyme, likely due to the production of thinner and less *O*-acetylated peptidoglycan. Using a suppressor screen, we show here that suppression of *eslB* phenotypes could be achieved by enhancing peptidoglycan biosynthesis, reducing peptidoglycan hydrolysis or alterations in WTA biosynthesis and modification. The lack of EslB also leads to a higher negative surface charge, which likely stimulates the activity of peptidoglycan hydrolases and lysozyme. Based on our results, we hypothesize that the portion of cell surface exposed WTA is increased in the *eslB* mutant due to the thinner peptidoglycan layer and that latter one could be caused by an impairment in UDP-*N*-acetylglucosamine (UDP-Glc*N*Ac) production or distribution.

Author summary

Listeria monocytogenes is intrinsically resistant towards the cell wall hydrolase lysozyme, which is part of the human defense system. One of the factors, which confer lysozyme resistance by a yet unknown mechanism, is the predicted ABC transporter EslABC. Based on the data presented in this study, we propose that the production or distribution of UDP-Glc*N*Ac is altered in the absence of EslB, which ultimately leads to a reduction in peptidoglycan production and an increased negative surface charge. This negative surface charge likely enhances the binding and activity of lysozyme and peptidoglycan hydrolases. Our study highlights the importance of a balance between peptidoglycan and WTA biosynthesis to maintain the cell surface charge and prevent cell lysis due to imbalanced peptidoglycan hydrolase activity.

Introduction

In recent years, antibiotic resistance became a serious threat for public health. One of the main targets of currently available antibiotics is the bacterial cell wall (Fig. 1). In Gram-positive bacteria, the cell wall consists of a thick layer of peptidoglycan and cell wall polymers, which are either tethered to the cell membrane or covalently linked to peptidoglycan and referred to as lipoteichoic (LTA) and wall teichoic acid (WTA), respectively. Peptidoglycan biosynthesis starts in the cytoplasm by the conversion of UDP-*N*-acetylglucosamine (UDP-Glc*N*Ac) to UDP-*N*-acetylmuramic acid (UDP-Mur*N*Ac) via MurA and MurB. The activity of the UDP-Glc*N*Ac 1-carboxyvinyltransferase MurA can be specifically inhibited by the antibiotic fosfomycin (Fig. 1)(1). In the subsequent steps, which are depicted in Figure 1, the peptidoglycan precursor lipid II is synthesized in the cytoplasm and transported across the membrane by the flippase MurJ (2–4). Lipid II is then incorporated into the growing glycan strand by members of the SEDS (shape, elongation, division, sporulation) protein family, namely RodA and FtsW, which act in concert with class B penicillin binding proteins (PBPs) that have a transpeptidase activity (5–7). Recent findings led to the conclusion that class A PBPs, which possess a glycosyltransferase and a transpeptidase domain, are mainly involved in filling gaps and/or repair defects in the peptidoglycan mesh, rather than being the main enzymes involved in peptidoglycan polymerization and crosslinking (5,8,9). The ability of bacterial cells to elongate and divide depends on the activity of peptidoglycan hydrolases. Two DL-endopeptidase, CwlO and LytE, are essential for cell elongation in *Bacillus subtilis*. In addition to its role in cell elongation, LytE is also involved in cell separation (10–12). Both enzymes cleave the peptide bond between D-glutamic acid and *meso*-diamino pimelic acid of the peptidoglycan peptide, thereby allowing the insertion of new peptidoglycan material (13). Lack of CwlO results in cell shortening, while absence of CwlO and LytE is lethal (14,15). Peptidoglycan biosynthesis and hydrolysis need to be tightly regulated to prevent cell lysis. In *B. subtilis*, this regulation is partly achieved by controlling expression of *cwlO* and *lytE* via the

75 essential two-component system WalRK, whose expression is for instance induced during heat
76 stress (16–18). On the other hand, activity of CwlO depends on a direct protein-protein
77 interaction with the ABC transporter FtsEX (19). The FtsEX-dependent regulation of *B. subtilis*
78 CwlO further depends on the presence of two cofactors, SweC and SweD (20,21).

79 UDP-Glc*N*Ac is synthesized from fructose-6-phosphate via a four-step reaction
80 catalyzed by GlmS, GlmM, GlmU and GlmR and serves as a substrate of MurA. Recent
81 findings suggest that the UDP-Glc*N*Ac biosynthetic pathway can be inhibited by *trans*-
82 cinnamaldehyde (*t*-Cin) (Fig. 1)(22,23). UDP-Glc*N*Ac is also consumed by TarO/TagO, which
83 catalyzes the first committed step for the synthesis of WTA (24). The activity of TarO/TagO
84 can be blocked by tunicamycin, which also affects the activity of MraY at high concentrations
85 (25–28). In *L. monocytogenes* 10403S, WTA is composed of a glucose-glucose(Glc-Glc)-
86 glycerol phosphate-Glc*N*Ac-*N*-acetylmannosamine (Man*N*Ac) linker unit and an anionic ribitol
87 phosphate backbone, which can be modified with rhamnose, Glc*N*Ac and D-alanine residues
88 (29). The modification of WTA with positively charged D-alanine residues helps to mask the
89 negative charge of the ribitol phosphate backbone, thereby conferring resistance towards
90 cationic antimicrobial peptides and lysozyme (30,31).

91 Lysozyme is an enzyme that cleaves the β-1,4-glycosidic bond between Mur*N*Ac and
92 Glc*N*Ac of the bacterial peptidoglycan backbone and is found in human body fluids such as
93 tears, saliva and mucus. *L. monocytogenes* is intrinsically resistant towards lysozyme, which
94 is mainly achieved by modifications of the peptidoglycan. PgdA, an *N*-deacetylase, and OatA,
95 an *O*-acetyltransferase, deacetylate and acetylate the Glc*N*Ac and Mur*N*Ac residues,
96 respectively (32,33). In addition to peptidoglycan modifying enzymes, lysozyme resistance of
97 *L. monocytogenes* is affected by the activity of the predicted carboxypeptidase PbpX, the non-
98 coding RNA Rli31 and the transcription factor DegU (34). Interestingly, it was also been
99 observed that the lack of components of the putative ABC transporter EslABC leads to a strong
100 reduction in lysozyme resistance (34–36). Recently, we could show that the absence of EslB,
101 one of the transmembrane proteins of the EslABC transporter, resulted in the production of a
102 thinner peptidoglycan layer and a reduction in *O*-acetylation of the peptidoglycan, which likely
103 contributes to the reduced lysozyme resistance. Additionally, we observed that the *eslB* mutant
104 is unable to grow in media containing high sugar concentrations and that the strain has a cell
105 division defect (21,36).

106 In the current study, we used a suppressor screen to gain further insights into the role
107 of EslABC on the physiology of *L. monocytogenes*. This screen revealed that phenotypes of
108 the *eslB* mutant can either be suppressed by enhancing peptidoglycan biosynthesis, reducing
109 peptidoglycan hydrolysis or by altering WTA production or modification. Using a cytochrome C
110 assay, we further demonstrate that the lack of EslB manifests in a higher negative surface

111 charge, which likely affects the activity of peptidoglycan hydrolases and provides an additional
112 explanation for the increased lysozyme sensitivity of the *eslB* mutant.
113
114 **Results**
115 **Δ*eslB* phenotypes are restored in the presence of excess Mg^{2+}**
116 The *eslABCR* operon encodes the putative ABC transporter EslABC and the RpiR
117 transcriptional regulator EslR. Absence of the transmembrane component EslB leads to a
118 multitude of phenotypes including a cell division defect, decreased lysozyme resistance, the
119 production of a thinner cell wall and a growth defect in media containing high sugar
120 concentrations (36). In addition, we observed that the growth of the *eslB* mutant is severely
121 affected when grown on BHI plates at 42°C (Fig. 3A). So far, the cellular function of the
122 transporter EslABC and how it is mechanistically linked to cell division and cell wall
123 biosynthesis in *L. monocytogenes* is unknown. Generally, many cell wall defects can be
124 rescued by the addition of Mg^{2+}, however, the reason for this is still debated. Recently, it was
125 speculated that binding of Mg^{2+} to the cell wall inhibits peptidoglycan hydrolases and thereby
126 stabilizes the bacterial cell wall (37). As the phenotypic defects of the *eslB* mutant suggest that
127 peptidoglycan biosynthesis might be impaired, we speculated that the addition of Mg^{2+} should
128 rescue the growth of this strain. To test this hypothesis, the *L. monocytogenes* wildtype
129 10403S, the Δ*eslB* mutant and the Δ*eslB* complementation strain were grown on BHI plates
130 containing sucrose and penicillin, lysozyme or were incubated at 42°C in the absence or
131 presence of 20 mM $MgCl_2$. The addition of Mg^{2+} could restore the growth of the Δ*eslB* mutant
132 under all conditions tested (Fig. S1), further supporting the hypothesis that peptidoglycan
133 biosynthesis is impaired in *L. monocytogenes* cells lacking EslB.
134
135 **Resistance profile of the *eslB* mutant towards cell wall-targeting antibiotics**
136 To narrow down which point of the peptidoglycan biosynthesis pathway is impaired in
137 the *eslB* mutant, we performed disk diffusion assays with antibiotics that target different steps
138 of this pathway (Fig. 1). Compared to the wildtype, the *eslB* mutant was more sensitive towards
139 *t*-Cin and fosfomycin (Fig. 2), which target the UDP-Glc*N*Ac biosynthetic pathway and MurA,
140 respectively (22,23,38). In contrast, the resistance towards D-cycloserine, nisin, vancomycin,
141 moenomycin, penicillin, ampicillin and bacitracin (Fig. 1), which target processes downstream
142 of MurA, was not altered in the *eslB* mutant (Fig. S2). The *eslB* mutant was more resistant
143 towards tunicamycin, whose main target at low concentrations is TarO, the first enzyme
144 functioning in the WTA biosynthesis pathway. As we have seen above, the inhibition of WTA
145 biosynthesis seems to be beneficial for the *eslB* mutant likely due to an increased flux of UDP-
146 Glc*N*Ac towards peptidoglycan biosynthesis. This antibiotic screen therefore suggests that one
147 of the limiting factors of the *eslB* mutant might be the synthesis or correct distribution of UDP-

148 Glc*N*Ac, a precursor, which is used for both peptidoglycan biosynthesis and the synthesis and
149 modification of WTA. This hypothesis is supported by the observation that overproduction of
150 GlmM and GlmR, two proteins involved in the production of UDP-Glc*N*Ac, can partially
151 suppress the *eslB* phenotypes (Fig. S3).
152
153 **Isolation of *eslB* suppressor mutants**
154 To gain insights into the function of EslABC, we took advantage of the observation that
155 the *eslB* mutant forms suppressors when grown on BHI plates that contain either 100 µg ml^{-1}
156 lysozyme, or 0.5 M sucrose and 0.025 or 0.05 µg ml^{-1} penicillin. Genomic alterations present
157 in independently isolated *eslB* suppressors were determined by whole genome sequencing. A
158 large subset of *eslB* suppressors had mutations in *walR* (*lmo0287*) or *walK* (*lmo0288*), which
159 encode the WalRK two-component system that is involved in cell wall metabolism (17,39). In
160 addition, we identified mutations that mapped to genes associated with peptidoglycan
161 biosynthesis (*murZ* (*lmo2552*), *reoM* (*lmo1503), prpC* (*lmo1821*), *pbpA1* (*lmo1892*)),
162 peptidoglycan hydrolysis (*cwlO* (*lmo2505, spl*), *ftsX* (*lmo2506*), *ftsE* (*lmo2507*)) and wall
163 teichoic acid (WTA) biosynthesis and modification (*tarL* (*lmo1077*), *dltX* (promoter region,
164 *lmrg_02074*)) (Table 1).
165

166 **Table 1: Identified sequence alterations in *L. monocytogenes eslB* deletion strains and suppressors.**

Strain number	Reference position[1]	Type[2]	Ref[3]	Allele[4]	Frequency[5]	Annotations[6]	AA change[7]	Condition[8]
ANG4275 10403SΔ*eslB*$_{(1)}$	2425786-2425875	DEL			100%	*lmo2396*, internalin	30 aa deletion	
ANG5386	2583855	DEL	T	-	100%	*murZ*, UDP-*N*-acetylglucosamine 1-carboxyvinyltransferase	M240fs	P
ANG5479	310043	SNV	G	A	100%	*walK*, histidine kinase of TCS WalRK	R553H	P
ANG5480	309234	SNV	C	G	100%	*walK*, histidine kinase of TCS WalRK	N283E	P
ANG5488	2537835	SNV	C	G	100%	*ftsX,* membrane component of ABC transporter FtsEX	G243R	P
ANG5489	310094	SNV	C	T	100%	*walK*, histidine kinase of TCS WalRK	A570V	P
ANG5499	1491251	DEL	T	-	100%	*reoM*, regulator of MurA degradation	L23fs	P
ANG5662 10403SΔ*eslB*$_{(2)}$	–							
ANG5698	2582654	DEL	G	-	100%	*murZ*, UDP-*N*-acetylglucosamine 1-carboxyvinyltransferase	Q307fs	P
ANG5699	310133	SNV	T	C	97.4%	*walK*, histidine kinase of TCS WalRK	I583T	P
ANG5708	1852252	SNV	G	A	100%	*prpC*, serine threonine phosphatase	P159L	P
ANG5710	2537273	SNV	C	T	98%	*cwlO*, peptidoglycan DL-endopeptidase	R106H	P
ANG5714	2538568	SNV	G	A	98.4%	*ftsE*, ATP binding protein of ABC transporter FtsEX	Q220-	P
ANG5733	308133	SNV	A	G	100%	*walR*, response regulator of TCS WalRK	S216G	L
ANG5734	309772	SNV	C	G	100%	*walK*, histidine kinase of TCS WalRK	H463D	L
ANG5737	309085	SNV	G	T	100%	*walK*, histidine kinase of TCS WalRK	V234L	L
ANG5741	309824	SNV	G	A	100%	*walK*, histidine kinase of TCS WalRK	R480H	L
ANG5685	–							

10403SΔ*eslB*[3]								
ANG5717	1921373	SNV	G	A	100%	*pbpA1*, bifunctional penicillin binding protein	G125D	P
ANG5729	1090622	SNV	C	T	100%	*tarL,* teichoic acid ribitol-phosphate polymerase	P282L	P
ANG5746	988580	SNV	T	C	100%	Promoter of *dlt* operon, involved in D-alanylation of wall teichoic and lipoteichoic acids	-	L

[1] Reference position is based on the position in the *L. monocytogenes* 10403S reference genome (NC_01744).

[2] Type of mutation: SNV = single nucleotide variant; DEL = nucleotide deletion.

[3] Ref indicates base in reference genome.

[4] Allele indicates base at the same position in the sequenced strain.

[5] Frequency at which the base change was found in the sequenced strain.

[6] AA change indicates the resulting amino acid change in the protein found in the reference strains as compared to the sequenced strain.

[7] TCS = Two-component system

[8] Condition, which was used to raise suppressors. L = BHI plates containing 100 µg/ml lysozyme. P = BHI plates containing 0.5 M sucrose and 0.025 or 0.05 µg/ml penicillin.

176 **Suppression of *eslB* phenotypes by increased MurA levels**

177 Under sucrose penicillin stress, two *eslB* suppressors with mutations in *murZ* and one
178 *eslB* suppressor with a mutation in *reoM* or *prpC* were isolated. The proteins encoded by all
179 three of these genes affect MurA protein levels (40,41). Drop dilution assays were performed
180 to assess, whether mutations in *murZ*, *reoM* and *prpC* suppress the growth defect of the *eslB*
181 mutant in the presence of sucrose and penicillin as well as other conditions under which the
182 growth of the *eslB* mutant is severely affected. As expected, the growth of the *L.*
183 *monocytogenes* strains 10403S∆$eslB_{(1)}$ $murZ^{M240fs}$, 10403S∆$eslB_{(2)}$ $murZ^{Q307fs}$, 10403S∆$eslB_{(1)}$
184 $reoM^{K23fs}$ and 10403S∆$eslB_{(2)}$ $prpC^{P159L}$ on BHI plates containing sucrose and penicillin is
185 comparable to the wildtype strain 10403S. The suppressors with mutations in *murZ*, *reoM* and
186 *prpC* also grew like wild-type on BHI plates containing lysozyme as well as on BHI plates that
187 were incubated at 42°C (Fig. 3A, data not shown).

188 MurZ is a homolog of the UDP-*N*-acetylglucosamine 1-carboxyvinyltransferase MurA,
189 which is required for the first step of peptidoglycan biosynthesis (Fig. 1)(42,43). While MurA is
190 essential for the growth of *L. monocytogenes*, the deletion of *murZ* is possible and results in
191 the stabilization of MurA (44). MurA is a substrate of the ClpCP protease and a recent study
192 showed that ReoM is required for the ClpCP-dependent proteolytic degradation of MurA in *L.*
193 *monocytogenes* (40,44). The activity of ReoM is controlled by the serine/threonine kinase PrkA
194 and the cognate phosphatase PrpC. The phosphorylated form of ReoM stimulates
195 peptidoglycan biosynthesis by preventing ClpCP-dependent degradation of MurA, while MurA
196 degradation is enhanced in the presence of non-phosphorylated ReoM (40,41). The identified
197 mutations in *murZ* and *reoM* in our suppressor strains lead to frameshifts, and thus to the
198 production of inactive MurZ and ReoM proteins. It has been previously shown that MurA protein
199 levels are increased in *murZ* and *reoM* mutants (40,44) and we thus assume that this is also
200 the case for the *eslB* suppressor strains 10403S∆$eslB_{(1)}$ $murZ^{M240fs}$, 10403S∆$eslB_{(2)}$ $murZ^{Q307fs}$
201 and 10403S∆$eslB_{(1)}$ $reoM^{K23fs}$. The identified mutation in *prpC* in the suppressor strain
202 10403S∆$eslB_{(2)}$ $prpC^{P159L}$ leads to the production of a variant of PrpC, in which proline at
203 position 159 is replaced by a leucine, however, it is currently not known whether this amino
204 acid exchange leads to decreased or enhanced activity of PrpC. A decreased activity of PrpC
205 would lead to accumulation of MurA (41), while enhanced activity would result in reduced MurA
206 levels. To assess which affect the P159L mutation in *prpC* has on MurA levels, western blots
207 were performed using a MurAA-specific antibody. Protein samples of *L. monocytogenes*
208 strains EGD-e and EGD-e ∆*clpC* were used as controls. In accordance with previous studies,
209 MurA accumulated in the *clpC* mutant (44). The production of the mutated PrpC variant,
210 $PrpC^{P159L}$, also led to a slight accumulation of MurA in the *eslB* mutant background (Fig. 3B).
211 Additionally, no change in MurA levels could be observed for the *eslB* mutant compared to the
212 wildtype strain 10403S (Fig 3B). These results suggest that while the decrease in

213 peptidoglycan production seen in the *eslB* mutant is not caused by decreased MurA levels, the
214 growth deficit of the *eslB* mutant can be rescued by preventing MurA degradation.
215 To confirm that the suppression of the *eslB* phenotypes in the strains with mutations in
216 *murZ*, *reoM* or *prpC* is indeed the result of increased MurA protein levels, we integrated a
217 second, IPTG-inducible copy of *murA* into the genome of the *eslB* mutant. First, we determined
218 the resistance towards fosfomycin, which is a known inhibitor of MurA (Fig. 4A-B)(1), for the *L.*
219 *monocytogenes* wildtype and the *eslB* mutant harboring the empty plasmid pIMK3 or pIMK3-
220 *murA* in the presence of IPTG. Strain 10403S∆*eslB* pIMK3 is three-fold more sensitive to
221 fosfomycin as compared to the cognate wildtype strain. The induction of *murA* expression
222 increases the resistance of strains 10403S pIMK3-*murA* and 10403S∆*eslB* pIMK3-*murA* (Fig.
223 4A-B), suggesting that MurA is indeed overproduced in these strains.
224 Next, we assessed whether the growth phenotypes of the *eslB* mutant can be
225 suppressed by the overexpression of *murA*. In the presence of the inducer IPTG, the growth
226 of strain 10403S∆*eslB* pIMK3-*murA* was comparable to the corresponding wildtype strain
227 under all conditions tested (Fig. 4C). These results indicate that overproduction of MurA can
228 compensate for the loss of *eslB* and that the suppression of the *eslB* phenotypes in the *murZ*,
229 *reoM* and *prpC* suppressors is likely the result of increased MurA levels.
230 Interestingly, increased MurA production also leads to the suppression of the cell
231 division defect of the *eslB* mutant. Cells of the *eslB* mutant carrying the empty pIMK3 plasmid
232 have a cell length of 3.19±0.29 µm. In contrast, strain 10403S∆*eslB* pIMK3-*murA* produces
233 cells with a length of 2.27±0.03 µm, a size that is comparable to the length of *L. monocytogenes*
234 wildtype cells (Fig. 4D-E).
235
236 **Suppression by reduction of the glycosyltransferase activity of PBP A1**
237 Multiple enzymes are involved in the production of lipid II, the peptidoglycan precursor,
238 within the cytoplasm. After its transport across the membrane via MurJ, lipid II is incorporated
239 into the growing glycan strand by glycosyltransferases, which can either be class A penicillin
240 binding proteins (PBPs), monofunctional glycosyltransferases or members of the SEDS
241 (shape, elongation, division, sporulation) family, such as RodA and FtsW (5,45,46). *L.*
242 *monocytogenes* encodes two class A PBPs, PBP A1 and PBP A2, in its genome (47,48). One
243 of the *eslB* suppressor strains, ANG5717, carries a point mutation in *pbpA1* leading to the
244 substitution of glycine at position 125 by aspartate. Interestingly, this glycine residue is part of
245 the catalytic site of the glycosyltransferase domain, suggesting that the glycosyltransferase
246 activity of the PBP A1 variant PBP A1^{G125D} might be reduced. Drop dilution assays and
247 microscopic analysis revealed that the phenotypes associated with deletion of *eslB* can be
248 rescued by *pbpA1*^{G125D} (Fig. 5A-C). The glycosyltransferase activity of class A PBPs can be
249 inhibited by moenomycin (49). We thus tested whether the presence of moenomycin would

250 enable the growth of the *eslB* mutant under heat stress. As shown in Figure 5D, the *eslB*
251 mutant is unable to grow at 42°C on BHI plates or BHI plates containing DMSO, which was
252 used to dissolve moenomycin. In contrast, nearly wildtype-like growth of the *eslB* mutant was
253 observed on BHI plates that were supplemented with moenomycin. These results suggest that
254 growth deficits of the *eslB* mutant can be rescued by the reduction of the glycosyltransferase
255 activity of class A PBPs.
256
257 **Suppression by reducing *cwlO* expression or CwlO activity**
258 In addition to suppressors associated with MurA and PBP A1, we isolated suppressors
259 carrying mutations in genes that either affect the transcription of *cwlO* or the activity of CwlO.
260 CwlO is a DL-endopeptidase, which opens the existing cell wall to allow for the insertion of
261 new lipid II precursors during cell elongation of *B. subtilis* (14,16). In *B. subtilis*, transcription
262 of *cwlO* is induced by WalRK in response to low DL-endopeptidase activity (16,17,50) and
263 CwlO activity is stimulated by a direct interaction with the ABC transporter FtsEX (19). In our
264 suppressor screen, we isolated eight *eslB* suppressor strains that carried mutations in *walK*,
265 which were either isolated under lysozyme or sucrose penicillin stress, and four *eslB*
266 suppressor strains that carried mutations in *walR* from which the majority was isolated in the
267 presence of lysozyme stress. We selected *eslB* suppressors 10403SΔ*eslB*$_{(2)}$ *walR*^{S216G}
268 and10403SΔ*eslB*$_{(2)}$ *walK*^{H463D}, which were isolated under lysozyme stress, and 10403SΔ*eslB*$_{(2)}$
269 *walK*^{I583T}, which was isolated under sucrose penicillin stress, for further analysis. In addition,
270 three suppressors with mutations were isolated in *ftsE*, *ftsX* and *cwlO* under sucrose penicillin
271 pressure (Table 1).
272 Spot plating assays showed that the *eslB* suppressors with mutations in either *walR* or
273 *walK* could overcome the growth defect of the *eslB* mutant under sucrose penicillin, lysozyme
274 and heat stress (Fig. 6). In contrast, *eslB* suppressors harboring mutations in either *ftsE*, *ftsX*
275 or *cwlO*, grow comparable to the wildtype under sucrose penicillin and heat stress, but showed
276 a similar growth defect as the *eslB* mutant on plates containing lysozyme (Fig. 6A). Microscopic
277 analysis of the *eslB* suppressors with mutations in *walR*, *walK*, *ftsE*, *ftsX* and *cwlO* revealed
278 that these cells have a similar cell length to the *L. monocytogenes* wildtype 10403S and thus,
279 the expression of mutated WalR, WalK, FtsE and CwlO variants could restore the cell division
280 defect of the *eslB* mutant (Fig. 6B-C). Additionally, we observed that the cells of suppressor
281 strains 10403SΔ*eslB*$_{(2)}$ *cwlO*^{R106H} and 10403SΔ*eslB*$_{(2)}$ *ftsE*$^{Q220-}$ were bent compared to the
282 wildtype strain. This phenotype is characteristic for *B. subtilis cwlO* and *ftsE* mutants (19,51)
283 suggesting that the acquired mutations in *cwlO* and *ftsE* led to inactivation or reduced activity
284 of CwlO and FtsE in *L. monocytogenes*.
285 The observation that mutations accumulate in genes associated with CwlO led to the
286 hypothesis that wildtype CwlO activity is toxic, due to the reduced peptidoglycan levels

287 produced by the *eslB* mutant (36). To confirm this hypothesis, an *eslB cwlO* double mutant
288 was constructed, in which the expression of an ectopic copy of *cwlO* was placed under the
289 control of an IPTG-inducible promoter. As expected, in the absence of the inducer, the *eslB*
290 *cwlO* double mutant was able to grow on BHI plates supplemented with sucrose and penicillin.
291 In accordance to the results obtained for the suppressors, the growth of a strain lacking both,
292 EslB and CwlO, was still impaired in the presence of lysozyme. Furthermore, individual deletion
293 of either *eslB* or *cwlO* resulted in a severe growth defect at higher temperatures, while the *eslB*
294 *cwlO* double mutant was able to grow in the absence of IPTG at 42°C. Induction of *cwlO*
295 expression in strain 10403S∆*cwlO* ∆*eslB* pIMK3-*cwlO* resulted in a growth defect under
296 sucrose penicillin and under heat stress, which is comparable to that of the *eslB* mutant (Fig.
297 7A). Next, we studied the cell morphology of strains lacking CwlO, EslB or both. In accordance
298 with previous studies investigating the function of CwlO in *B. subtilis* (19,51), the *L.*
299 *moncytogenes cwlO* mutant formed slightly smaller, bent cells (Fig.7B-C). Cells lacking both,
300 EslB and CwlO, were also shorter than cells of the *L. monocytogenes* wildtype 10403S, while
301 induction of *cwlO* expression in strain 10403S∆*cwlO* ∆*eslB* pIMK3-*cwlO* resulted in the
302 formation of elongated cells (Fig. 7B-C). Altogether, these findings support our hypothesis that
303 the suppression of the *eslB* phenotypes in the *cwlO*, *ftsE* and *ftsX* suppressors is the result of
304 an inactivation of the DL-endopeptidase CwlO.
305
306 **Suppression by inhibition of WTA biosynthesis**
307 In *B. subtilis,* WalRK does not only stimulate transcription of *cwlO,* but also of the *tagAB*
308 and *tagDEFGH* operons, which encode proteins required for WTA biosynthesis and export
309 (39). In *L. monocytogenes* 10403S, WTA is composed of a ribitol phosphate backbone, which
310 is attached to a Glc-Glc-glycerol phosphate-Glc*N*Ac-Man*N*Ac linker unit and modified with
311 Glc*N*Ac, rhamnose and D-alanine residues (29,30). Thus, UDP-Glc*N*Ac is consumed by
312 several enzymes during WTA biosynthesis and modification. As mentioned above, we isolated
313 suppressors containing mutations in *lmo1077,* encoding a TarL homolog, and the promoter
314 region of the *dlt* operon (Table 1). TarL is a teichoic acid ribitol phosphate polymerase required
315 for the polymerization of the ribitol phosphate backbone of WTA (Fig. 1)(30). The *dlt* operon
316 codes for proteins that are essential for the D-alanylation of WTA (52–54). Figure 8A shows
317 that the *eslB* mutant, which harbors a mutation in *tarL,* could grow again under sucrose
318 penicillin and lysozyme stress, likely due to a reduction in WTA biosynthesis and potentially
319 leading to an increase in the cellular UDP-Glc*N*Ac pool, which can then be used by MurA.
320 However, the *tarL* suppressor is unable to grow at 42°C. A similar phenotype could be
321 observed when the *L. monocytogenes* wildtype strain 10403S is grown at 42°C on a plate
322 containing high concentrations of tunicamycin, which inhibits TarO, the first enzyme required
323 for WTA biosynthesis (data not shown). This indicates that the mutated TarL variant produced

324 by the *eslB* suppressor strain ANG5729 has a reduced activity. To further test if inhibition of
325 WTA biosynthesis is indeed beneficial for the *eslB* mutant, we grew the *eslB* mutant at 42°C
326 on BHI plates containing different concentrations of tunicamycin. We could see partial
327 suppression of the heat sensitivity at a tunicamycin concentration of 0.05 µg/ml and the *eslB*
328 mutant grew comparable to the *L. monocytogenes* wildtype strain 10403S and the
329 complementation strain on plates containing 0.5 µg/ml tunicamycin (Fig. S4). These results
330 demonstrate that reduction of WTA biosynthesis leads to the suppression of the heat
331 phenotype associated of the *eslB* mutant.

332 Figure 8A further shows that the *eslB* suppressor strain, which harbors a mutation in the
333 *dlt* promoter region, could grow again under all conditions tested. To assess what consequence
334 the point mutation in the promoter region of the *dlt* operon has on gene expression, we place
335 the promoterless *lacZ* gene under the control of the *dlt* promoter or the mutated *dlt* promoter
336 found in suppressor strain ANG5746. The *lacZ* promotor gene fusions were introduced into *B.*
337 *subtilis* and β-galactosidase activities determined. This analysis showed that the mutation in
338 the *dlt* promoter resulted in increased promoter activity and likely increased D-alanylation of
339 teichoic acids in the suppressor strain (Fig. 8B). The D-alanylation state of teichoic acids is an
340 important factor that impacts the bacterial cell surface charge (31). As we isolated a suppressor
341 that increased the expression of the *dlt* operon, we wondered, whether the surface charge of
342 *eslB* mutant cells is altered. To test this, we determined the binding capability of positively
343 charged cytochrome C to the cell surface of different *L. monocytogenes* strains, which serves
344 as a readout of the bacterial surface charge (55,56). A strain lacking D-alanine residues on
345 LTA and WTA due to a deletion of *dltA* was used as a control. As expected, the cell surface of
346 the *dltA* mutant had a higher negative charge as compared to the *L. monocytogenes* wildtype
347 strain 10403S. A similar result was observed for the *eslB* mutant. The high negative surface
348 charge of the *eslB* mutant could be partially rescued by the mutation in the *dlt* promoter, which
349 is present in the *eslB* suppressor strain 10403SΔ*eslB* P_{dlt}* (Fig. 8C). This result suggests that
350 either the D-alanylation state of WTAs is altered in the absence of EslB or that the surface
351 presentation of WTA is changed due to the production of a thinner peptidoglycan layer.

352

353 **Discussion**

354 In this study, we aimed to provide further insight into the connection between the
355 predicted ABC transporter EslABC and peptidoglycan biosynthesis. Previous studies have
356 shown that the deletion of *eslB*, coding for one of transmembrane components of the
357 transporter, leads to a growth defect on sucrose containing media, the formation of elongated
358 cells, the production of a thinner peptidoglycan layer, as well as sensitivity towards the natural
359 antibiotic lysozyme and cationic antimicrobial peptides (34–36), suggesting its involvement in
360 peptidoglycan biosynthesis and cell division. It was proposed that the addition of Mg^{2+} rescues

361 mutants with a defect in peptidoglycan biosynthesis by reducing the activity of peptidoglycan
362 hydrolases (37). In accordance with this, we observed a suppression of the *eslB* growth deficits
363 under all conditions tested when an excess of Mg^{2+} was added. *L. monocytogenes* encodes
364 several peptidoglycan hydrolases, including the DL-endopeptidase CwlO (SpI), the LytM-
365 domain containing protein Lmo2504 and the two cell wall hydrolases NamA and CwhA (p60),
366 which are required for daughter cell separation (57,58). We have isolated several *eslB*
367 suppressors, which carry mutations in *cwlO* or mutations in other genes, e.g. *ftsE* or *ftsX*, which
368 affect CwlO activity. After depletion of CwlO, the *eslB* mutant was able to grow in otherwise
369 non-permissive conditions, suggesting that the activity of CwlO might be deregulated in the
370 *eslB* deletion strain or that the peptidoglycan of the *eslB* mutant is more sensitive to hydrolysis
371 by CwlO. CwlO activity is controlled by a direct protein-protein interaction with the ABC
372 transporter FtsEX (19). It is thus tempting to speculate that the ABC transporter EslABC might
373 also affect CwlO activity or localization of proteins involved in peptidoglycan biosynthesis
374 and/or degradation. Interestingly, a strain lacking both EslB and CwlO is able to grow at
375 elevated temperatures, while both single mutants are not able to grow under this condition.
376 We could isolate *eslB* suppressor strains with mutations that are associated with
377 stabilization of MurA, the UDP-Glc*N*Ac 1-carboxyvinyltransferase responsible for the first step
378 of peptidoglycan biosynthesis. Elevated levels of MurA, and thus, enhanced peptidoglycan
379 biosynthesis could fully restore the phenotypic defects of the 10403S∆*eslB* strain. To identify
380 the exact process of peptidoglycan biosynthesis, which is impaired in the *eslB* mutant, we
381 performed a screen with antibiotics targeting different steps of this process. The absence of
382 *eslB* only affected the resistance towards *t*-Cin and fosfomycin, which reduce the synthesis of
383 UDP-Glc*N*Ac and inhibit MurA, respectively (22,23,38). Surprisingly, we observed an
384 increased resistance of the *eslB* mutant towards tunicamycin. The primary target of
385 tunicamycin is TarO, the first enzyme of WTA biosynthesis, and, at high concentrations, also
386 MraY, which is responsible for the production of lipid I during peptidoglycan biosynthesis (Fig.
387 1)(25–28). During WTA biosynthesis, UDP-Glc*N*Ac is used for the synthesis of the linker unit
388 and for the modification of the WTA backbone (29,59,60). Thus, reducing the production of
389 WTA could increase the availability of UDP-Glc*N*Ac for peptidoglycan biosynthesis and
390 therefore support the growth of the *eslB* mutant under non-permissive conditions. In
391 accordance with this, we observed a partial suppression of the *eslB* phenotypes by the
392 overproduction of GlmM and GlmR, two enzymes required for the synthesis of UDP-Glc*N*Ac
393 (22). These results suggest that either the production or distribution of UDP-Glc*N*Ac as a
394 substrate between different pathways might be disturbed in the *eslB* mutant.
395 Cell wall stability depends on the balance between peptidoglycan biosynthesis and
396 hydrolysis. An imbalance of one of these processes results in rapid cell lysis (61). Recent
397 studies suggest that new peptidoglycan precursors are inserted into the growing glycan chains

398 by the Rod system, which is composed of several enzymes. In contrast, class A PBPs are
399 thought to fill gaps and/or repair cell wall defects (5,8,9). It was recently shown that enhanced
400 endopeptidase activity leads to the activation of class A PBPs in *E. coli* (62). A similar
401 mechanism seems to exist in *B. subtilis*, as either inactivation of PBP1 or inhibition of
402 peptidoglycan hydrolases by the addition of Mg^{2+} suppresses growth and morphological
403 defects of an *mreB* mutant (37). In accordance with this, we also observed suppression of the
404 heat sensitivity of the *eslB* mutant in presence of moenomycin, which specifically inhibits the
405 glycosyltransferase activity of class A PBPs (63,64).
406 In our suppressor screen, we identified a strain carrying a mutation in the *dlt* promoter
407 region, which leads to an overproduction of the Dlt enzymes. These enzymes are required for
408 the modification of teichoic acids (TAs) with D-alanines (53,54,65). The modification of TAs
409 with D-alanine residues leads to a reduction in the negative surface charge and affects the
410 activity of peptidoglycan hydrolases (30,31,37). Furthermore, lack of D-alanine modifications
411 of TAs was shown to increase lysozyme sensitivity in *Staphylococcus aureus* (66).
412 Interestingly, the cell surface of the *eslB* mutant is more negatively charged, similar to that of
413 a strain lacking D-alanine modifications on TAs. Based on our results, we propose the following
414 model: The absence of EslB seems to affect the production and/or distribution of UDP-Glc*N*Ac
415 between different pathways, leading to the production of a thinner peptidoglycan layer. The
416 reduced peptidoglycan thickness could subsequently result in the presentation of a larger
417 portion of WTA on the bacterial cell surface, which would explain the higher negative surface
418 charge (Fig. 9). This higher negative surface charge would enhance the binding capability
419 and/or activity of cationic antimicrobial peptides, lysozyme as well as peptidoglycan hydrolases
420 (53,67–70) and furthermore explain the sensitivity of the *eslB* mutant towards CwlO activity,
421 lysozyme and cationic antimicrobial peptides (34,36).
422 The essential two-component system WalRK stimulates the transcription of several
423 peptidoglycan hydrolases in Gram-positive bacteria (17,39,71–73). In *B. subtilis*, WalRK also
424 regulates the expression of genes involved in WTA biosynthesis and export (39). The regulon
425 of the WalRK system has not yet been determined for *L. monocytogenes*, however, it was
426 shown that the system is essential (74). Inactivation of WalRK usually leads to cell death of
427 wildtype cells due to loss of peptidoglycan hydrolase activity, however, cell death could be
428 prevented by the inhibition of peptidoglycan biosynthesis (75). We have isolated several *eslB*
429 suppressors with mutations in *walR* and *walK*. As it is unlikely that all of these mutations are
430 gain-of-function mutations, we hypothesize that these mutations result in a reduced activity of
431 the WalRK system. This would lead to a reduced peptidoglycan hydrolase activity as well as a
432 reduction in WTA content, and reduction of the latter would at least partially restore the
433 bacterial cell surface charge of the *eslB* mutant.

434 Taken together, we could show that the lack of EslB results in a defect in peptidoglycan
435 biosynthesis, which can be suppressed by modulating the activity of enzymes involved in either
436 peptidoglycan biosynthesis or hydrolysis. Our results suggest that the production or distribution
437 of the peptidoglycan precursor UDP-Glc*N*Ac between different pathways might be disturbed in
438 the *eslB* mutant. Further studies are required to prove this hypothesis and to determine the
439 function of the ABC transporter EslABC.
440
441 **Materials and Methods**
442 **Bacterial Strains and growth conditions.** All strains and plasmids used in this study are
443 listed in Table S1. *Escherichia coli* strains were grown in Luria-Bertani (LB) medium and
444 *Listeria monocytogenes* strains in brain heart infusion (BHI) medium at 37°C unless otherwise
445 stated. Where required, antibiotics and supplements were added to the medium at the following
446 concentrations: for *E. coli* cultures, ampicillin (Amp) at 100 µg ml^{-1}, kanamycin (Kan) at 30 µg
447 ml^{-1}, and for *L. monocytogenes* cultures, chloramphenicol (Cam) at 10 µg ml^{-1}, erythromycin
448 (Erm) at 5 µg ml^{-1}, Kan at 30 µg ml^{-1}, nalidixic acid (Nal) at 30 µg ml^{-1}, streptomycin (Strep) at
449 200 µg ml^{-1} and IPTG at 1 mM.
450
451 **Strain and plasmid construction.** All primers used in this study are listed in Table S2. For
452 the construction of pIMK3-*murA*, pIMK3-*glmR*, pIMK3-*glmU* and pIMK3-*glmM*, the *murA*,
453 *glmR*, *glmU* and *glmM* genes were amplified using primer pairs JR90/JR91, JR134/JR135,
454 JR136/JR137 and JR138/JR139, respectively, cut with *Nco*I and *Sal*I and ligated into plasmid
455 pIMK3 that had been cut with the same enzymes. The resulting plasmids pIMK3-*murA,* pIMK3-
456 *glmR*, pIMK3-*glmU* and pIMK3-*glmM* were recovered in *E. coli* XL1-Blue yielding strains
457 EJR52, EJR106, EJR107 and EJR108. Next, plasmids pIMK3-*murA,* pIMK3-*glmR*, pIMK3-
458 *glmU* and pIMK3-*glmM* were transformed into *E. coli* S17-1 yielding strains EJR59, EJR132,
459 EJR133 and EJR134. Strain EJR59 was used as a donor strain to transfer plasmid pIMK3-
460 *murA* by conjugation into *L. monocytogenes* strains 10403S (ANG1263) and 10403S∆$eslB_{(2)}$
461 (ANG5662) using a previously described method (76). This resulted in the construction of
462 strains 10403S pIMK3-*murA* (LJR26) and 10403S∆$eslB_{(2)}$ pIMK3-*murA* (LJR27), in which the
463 expression of *murA* is under the control of an IPTG-inducible promoter. Strains carrying the
464 empty pIMK3 vector were used as controls. For this purpose, pIMK3 was transformed into *E.*
465 *coli* S17-1 yielding strain EJR58. S17-1 pIMK3 was subsequently used as a donor strain to
466 transfer plasmid pIMK3 by conjugation into *L. monocytogenes* strains 10403S (ANG1263) and
467 10403S∆$eslB_{(2)}$ (ANG5662), which resulted in the construction of strains 10403S pIMK3
468 (LJR24) and 10403S∆$eslB_{(2)}$ pIMK3 (LJR25). For the construction of pIMK3-*glmS*, the *glmS*
469 gene was amplified using primer pair JR140/JR141. The resulting PCR product was cut with
470 *BamH*I and *Xma*I and ligated into plasmid pIMK3 that had been cut with the same enzymes.

471 Plasmid pIMK3-*glmS* was recovered in *E. coli* XL1-Blue and subsequently transformed into *E.*
472 *coli* S17-1 yielding strains EJR112 and EJR135, respectively. Strains EJR132, EJR133,
473 EJR134 and EJR135 were used to transfer plasmids pIMK3-*glmR*, pIMK3-*glmU*, pIMK3-*glmM*
474 and pIMK3-*glmS* by conjugation into *L. monocytogenes* strain 10403S∆*eslB*$_{(2)}$ (ANG5662)
475 yielding strains 10403S∆*eslB*$_{(2)}$ pIMK3-*glmR* (LJR63), 10403S∆*eslB*$_{(2)}$ pIMK3-*glmU* (LJR64),
476 10403S∆*eslB*$_{(2)}$ pIMK3-*glmM* (LJR65) and 10403S∆*eslB*$_{(2)}$ pIMK3-*glmS* (LJR66).
477 For the construction of a markerless deletion of *cwlO* (*lmrg_01743*), 1-kb DNA
478 fragments up- and downstream of *cwlO* were amplified by PCR with primers LMS106/107 and
479 LMS104/105. The resulting PCR products were fused in a second PCR using primers
480 LMS105/106, the product cut with *BamH*I and *Kpn*I and ligated into pKSV7 that had been cut
481 with the same enzymes. The resulting plasmid pKSV7-∆*cwlO* was recovered in *E. coli* XL1-
482 Blue yielding strain EJR63. Plasmid pKSV7-∆*cwlO* was subsequently transformed into *L.*
483 *monocytogenes* 10403S and *cwlO* deleted by allelic exchange according to a previously
484 published method (77) yielding strain 10403S∆*cwlO* (LJR37). Since attempts of producing
485 electrocompetent *cwlO* cells were unsuccessful, plasmid pIMK3-*cwlO* was first conjugated into
486 strain LJR37, which allows for IPTG-inducible expression of *cwlO*, and resulting in the
487 construction of strain LJR103. For the construction of pIMK3-*cwlO*, *cwlO* was amplified using
488 the primer pair LMS226 and LMS227. The fragment was cut with *Nco*I and *BamH*I, ligated into
489 pIMK3 that had been cut with the same enzymes and recovered in *E. coli* XL1-blue and S17-
490 1, yielding strains EJR114 and EJR115, respectively. To generate a *cwlO eslB* double mutant,
491 plasmid pKSV7-∆*eslB* was first transformed into *L. monocytogenes* strain LJR103 resulting in
492 strain LJR114. The *eslB* gene was then deleted by allelic exchange. This resulted in the
493 construction of strain 10403S∆*cwlO* ∆*eslB* pIMK3-*cwlO* (LJR119).
494 For the construction of promoter-*lacZ* fusions, the plasmid pAC7 was used. The
495 promoter region of the *dlt* operon was amplified from genomic DNA of the *L. monocytogenes*
496 wildtype 10403S and the *eslB* suppressor strain ANG5746 containing a mutation 31 bp
497 upstream of the ATG start codon, using the primer pair LMS93 and LMS94. The PCR products
498 were digested with BamHI and EcoRI and ligated into pAC7. The resulting plasmids pAC7-P$_{dlt}$
499 and pAC7-P$_{dlt}$* were recovered in XL1 Blue resulting in strains EJR50 and EJR51.
500 Subsequently, both plasmids were integrated into the *amyE* site of the *B. subtilis* wildtype strain
501 168, resulting in strains BLMS4 and BLMS5, respectively.
502
503 **Generation of *eslB* suppressors and whole genome sequencing.** For the generation of
504 *eslB* suppressors, overnight cultures of three independently generated *L. monocytogenes eslB*
505 mutants, strains 10403S∆*eslB*$_{(1)}$ (ANG4275), 10403S∆*eslB*$_{(2)}$ (ANG5662) and 10403S∆*eslB*$_{(3)}$
506 (ANG5685), were adjusted to an OD_{600} of 1. 100 µl of 10^{-1} and 10^{-2} dilutions of these cultures
507 were plated on BHI plates containing (A) 0.5 M sucrose and 0.025 µg ml^{-1} penicillin, (B) 0.5 M

508 sucrose and 0.05 µg ml^{-1} penicillin or (C) 100 µg ml^{-1} lysozyme, conditions under which the
509 *eslB* mutant is unable to grow while the *L. monocytogenes* wildtype strain 10403S can grow.
510 The plates were incubated at 37°C overnight and single colonies were re-streaked on BHI
511 plates. This procedure was repeated at least three independent times per condition. The
512 genome sequence of a selection of *eslB* suppressors was determined by whole genome
513 sequencing (WGS) using an Illumina MiSeq machine and a 150 paired end Illumina kit as
514 described previously (36). The reads were trimmed, mapped to the *L. monocytogenes* 10403S
515 reference genome (NC_017544) and single nucleotide polymorphisms (SNPs) with a
516 frequency of at least 90% identified using CLC workbench genomics (Qiagen) and Geneious
517 Prime® v.2021.0.1. The whole genome sequencing data were deposited at the European
518 Nucleotide Archive (ENA) under accession number PRJEB55822.
519
520 **Determination of resistance towards antimicrobials.** For the disk diffusion assays,
521 overnight cultures of the indicated *L. monocytogenes* strains were adjusted to an OD_{600} of 0.1.
522 100 µl of cultures were spread on BHI agar plates using a cotton swap. Plates contained 1 mM
523 IPTG were indicated. 6 mm filter disks were placed on top of the agar surface, soaked with 20
524 µl of the appropriate antibiotic stock solution and the plates were incubated at 37°C. The
525 diameter of the inhibition zone was measured the next day. The following stock solutions were
526 used: 50 mg ml^{-1} fosfomycin, 1 mg ml^{-1} *t*-Cin, 5 mg ml^{-1} tunicamycin, 15 mg ml^{-1} D-cycloserine,
527 60 mg ml^{-1} nisin, 30 mg ml^{-1} vancomycin, 5 mg ml^{-1} moenomycin, 1 mg ml^{-1} penicillin, 10 mg
528 ml^{-1} ampicillin and 250 mg ml^{-1} bacitracin.
529
530 **Spot plating assays.** Overnight cultures of *L. monocytogenes* strains were adjusted to an
531 OD_{600} of 1 and serially diluted to 10^{-6}. 5 µl of each dilution were spotted on BHI agar plates,
532 BHI agar plates containing 0.5 M sucrose and 0.025 µg ml^{-1} penicillin; 100 µg ml^{-1} lysozyme;
533 0.025 µg/ml moenomycin, 500 µl DMSO, 0.05 µg ml^{-1} or 0.5 µg ml^{-1} tunicamycin and plates
534 incubated at 37°C unless otherwise stated. Where indicated, plates were supplemented with
535 1 mM IPTG or 20 mM $MgCl_2$. Images of plates were taken after 20-24 hours of incubation.
536
537 **Cell length analysis.** Overnight cultures of the indicated *L. monocytogenes* strains were
538 inoculated to an OD_{600} of 0.1 and grown to an OD_{600} of 0.3-0.6 at 37°C with agitation in BHI
539 medium or BHI medium containing 1 mM IPTG and the appropriate antibiotic. To stain the
540 bacterial membranes, 800 µl of the bacterial cultures were mixed with 40 µl of 100 µg ml^{-1} nile
541 red and incubated for 20 min at 37°C. The cells were washed twice in PBS buffer and
542 subsequently re-suspended in the same buffer. Cells were then fixed in 1.12%
543 paraformaldehyde for 20 min at room temperature in the dark and 1-1.5 µl of the cell
544 suspension was spotted on microscope slides covered with a thin agarose layer (1.5% in

545 ddH_2O). Phase contrast and fluorescence images were taken using a Zeiss Axioskop 40
546 microscope equipped with an EC Plan-NEOFLUAR 100X/1.3 objective (Carl Zeiss, Göttingen,
547 Germany) and coupled to an AxioCam MRm camera. Filter set 43 was used for the detection
548 of the nile red signal. The images were processed using the Axio Vision software (release 4.7).
549 The length of 50 cells per replicate was measured for each strain and the mean calculated.
550 Statistical analysis was performed using the software GraphPad Prism (version 8).
551
552 **Isolation of cellular proteins and western blotting.** Bacteria from a 20 ml culture were
553 harvested by centrifugation and washed with ZAP buffer (10 mM Tris-HCl, pH 7.5, 200 mM
554 NaCl). The cells were subsequently resuspended in 1 ml ZAP buffer containing 1 mM PMSF
555 and disrupted by sonication. Cellular debris was removed by centrifugation, the resulting
556 supernatant collected and separated by SDS polyacrylamide gel electrophoresis (PAGE).
557 Proteins were transferred onto positively charged polyvinylidene fluoride (PVDF) membranes
558 using a semi-dry transfer unit. MurA was detected using a polyclonal rabbit antiserum raised
559 against the *B. subtilis* MurAA protein (43), which also cross reacts with the *L. monocytogenes*
560 MurA protein, as primary antibody and an anti-rabbit immunoglobulin G conjugated to
561 horseradish peroxidase antibody as the secondary antibody. Blots were developed using ECL
562 chemiluminescence reagents (Thermo Scientific) and imaged using a chemiluminescence
563 imager (Vilber Lourmat).
564
565 **Cytochrome C binding assay.** Cytochrome C binding assays were performed as previously
566 described (78). Briefly, overnight cultures of *L. monocytogenes* were used to inoculated fresh
567 cultures to an OD_{600} of 0.05 in 4 ml BHI medium and the cultures were grown to an OD_{600} of
568 0.6-0.8 at 37°C and 200 rpm. Bacteria from 2 ml of the culture were harvested by centrifugation
569 at 16.200 x g for 1 min. Cells were then washed twice with 20 mM MOPS (3-(N morpholino)
570 propanesulfonic acid) buffer (pH 7) and adjusted to an OD_{600} of 0.25 in the same buffer.
571 Cytochrome C was added at a final concentration of 50 µg ml^{-1} and the suspension was
572 incubated in the dark for 10 min at room temperature. The suspension was centrifuged for 5
573 min at 16.200 x g, the supernatant removed and the absorbance of the supernatant was
574 measured at 410 nm (OD_{410} + cells). A reaction without cells was used as blank (OD_{410} – cells).
575 The percentage of bound cytochrome C was calculated as follows:
576 $$\% \text{ cytochrome C bound} = 100 - [(OD_{410} + \text{cells}) / (OD_{410} - \text{cells})$$
577
578 **β-galactosidase assay.** To compare the *dlt* promoter activity of the *L. monocytogenes*
579 wildtype and suppressor strain ANG5746, β-galactosidase assays were performed. For this
580 purpose, promoter-*lacZ* fusions were integrated into the *amyE* locus of *B. subtilis* 168. The
581 resulting *B. subtilis* strains were grown in CSE-glucose minimal medium at 37°C to an OD_{600}

582 of 0.5-0.8, bacteria from a culture aliquot harvested and the β-galactosidase activity
583 determined as described previously (79).
584

585 **Acknowledgements**

586 We thank Ivan Andrew and Jaspreet Haywood from the CSC Genomics Laboratory,
587 Hammersmith Hospital, for their help with the whole genome sequencing and Annika Gillis for
588 help with genome sequence analysis. We also thank Julia Busse for technical assistance and
589 Tayfun Acar for the help with some experiments. We are grateful to Prof. Jörg Stülke for
590 providing JR and LMS with laboratory space, equipment and consumables and to the
591 Göttingen Center for Molecular Biosciences (GZMB) for financial support. This work was
592 funded by the Wellcome Trust grant 210671/Z/18/Z and MRC grant MR/P011071/1 to AG, the
593 German research foundation (DFG) grants RI 2920/1-1 and RI 2920/2-1 to JR, HA 6830/4 to
594 SH. LMS was supported by the Göttingen Graduate School for Neurosciences, Biophysics,
595 and Molecular Biosciences (GGNB, DFG grant GSC226/4).
596

597 **References**

598 1. Kahan FM, Kahan JS, Cassidy PJ, Kropp H. The mechanism of action of fosfomycin
599 (phosphonomycin). Ann N Y Acad Sci. 1974 May;235(0):364–86.
600 2. Sham L-T, Butler EK, Lebar MD, Kahne D, Bernhardt TG, Ruiz N. Bacterial cell wall.
601 MurJ is the flippase of lipid-linked precursors for peptidoglycan biogenesis. Science.
602 2014 Jul;345(6193):220–2.
603 3. Meeske AJ, Sham L-T, Kimsey H, Koo B-M, Gross CA, Bernhardt TG, et al. MurJ and
604 a novel lipid II flippase are required for cell wall biogenesis in *Bacillus subtilis*. Proc Natl
605 Acad Sci. 2015 May 19;112(20):6437–42. Available from:
606 http://www.pnas.org/lookup/doi/10.1073/pnas.1504967112
607 4. Ruiz N. Bioinformatics identification of MurJ (MviN) as the peptidoglycan lipid II flippase
608 in *Escherichia coli*. Proc Natl Acad Sci U S A. 2008 Oct;105(40):15553–7.
609 5. Cho H, Wivagg CN, Kapoor M, Barry Z, Rohs PDA, Suh H, et al. Bacterial cell wall
610 biogenesis is mediated by SEDS and PBP polymerase families functioning semi-
611 autonomously. Nat Microbiol. 2016 Sep;1:16172.
612 6. Taguchi A, Welsh MA, Marmont LS, Lee W, Sjodt M, Kruse AC, et al. FtsW is a
613 peptidoglycan polymerase that is functional only in complex with its cognate penicillin-
614 binding protein. Nat Microbiol. 2019 Apr;4(4):587–94.
615 7. Leclercq S, Derouaux A, Olatunji S, Fraipont C, Egan AJF, Vollmer W, et al. Interplay
616 between penicillin-binding proteins and SEDS proteins promotes bacterial cell wall
617 synthesis. Sci Rep. 2017 Feb;7:43306.
618 8. Dion MF, Kapoor M, Sun Y, Wilson S, Ryan J, Vigouroux A, et al. *Bacillus subtilis* cell

619 diameter is determined by the opposing actions of two distinct cell wall synthetic
620 systems. Nat Microbiol. 2019 Aug;4(8):1294–305.
621 9. Vigouroux A, Cordier B, Aristov A, Alvarez L, Özbaykal G, Chaze T, et al. Class-A
622 penicillin binding proteins do not contribute to cell shape but repair cell-wall defects.
623 Elife. 2020 Jan 6;9:e51998. Available from: https://elifesciences.org/articles/51998
624 10. Ohnishi R, Ishikawa S, Sekiguchi J. Peptidoglycan hydrolase LytF plays a role in cell
625 separation with CwlF during vegetative growth of *Bacillus subtilis*. J Bacteriol. 1999
626 May;181(10):3178–84.
627 11. Vollmer W, Joris B, Charlier P, Foster S. Bacterial peptidoglycan (murein) hydrolases.
628 FEMS Microbiol Rev. 2008 Mar;32(2):259–86.
629 12. Carballido-López R, Formstone A, Li Y, Ehrlich SD, Noirot P, Errington J. Actin homolog
630 MreBH governs cell morphogenesis by localization of the cell wall hydrolase LytE. Dev
631 Cell. 2006 Sep;11(3):399–409.
632 13. Yamaguchi H, Furuhata K, Fukushima T, Yamamoto H, Sekiguchi J. Characterization
633 of a new *Bacillus subtilis* peptidoglycan hydrolase Gene, *yvcE* (named *cwlO*), and the
634 enzymatic properties of its encoded protein. J Biosci Bioeng. 2004;98(3):174–81.
635 Available from: http://joi.jlc.jst.go.jp/JST.JSTAGE/jbb/98.174?from=CrossRef
636 14. Hashimoto M, Ooiwa S, Sekiguchi J. Synthetic lethality of the *lytE cwlO* genotype in
637 *Bacillus subtilis* is caused by lack of D,L-endopeptidase activity at the lateral cell wall. J
638 Bacteriol. 2012 Feb 15;194(4):796–803. Available from:
639 https://jb.asm.org/content/194/4/796
640 15. Domínguez-Cuevas P, Porcelli I, Daniel RA, Errington J. Differentiated roles for MreB-
641 actin isologues and autolytic enzymes in *Bacillus subtilis* morphogenesis. Mol Microbiol.
642 2013 Sep;89(6):1084–98.
643 16. Bisicchia P, Noone D, Lioliou E, Howell A, Quigley S, Jensen T, et al. The essential
644 YycFG two-component system controls cell wall metabolism in *Bacillus subtilis*. Mol
645 Microbiol. 2007 Jul;65(1):180–200. Available from: http://doi.wiley.com/10.1111/j.1365-
646 2958.2007.05782.x
647 17. Dubrac S, Bisicchia P, Devine KM, Msadek T. A matter of life and death: cell wall
648 homeostasis and the WalKR (YycGF) essential signal transduction pathway. Mol
649 Microbiol. 2008 Dec;70(6):1307–22. Available from:
650 http://doi.wiley.com/10.1111/j.1365-2958.2008.06483.x
651 18. Takada H, Shiwa Y, Takino Y, Osaka N, Ueda S, Watanabe S, et al. Essentiality of
652 WalRK for growth in *Bacillus subtilis* and its role during heat stress. Microbiology. 2018
653 Apr;164(4):670–84.
654 19. Meisner J, Montero Llopis P, Sham L-T, Garner E, Bernhardt TG, Rudner DZ. FtsEX is
655 required for CwlO peptidoglycan hydrolase activity during cell wall elongation in *Bacillus*

656 *subtilis*. Mol Microbiol. 2013 Sep;89(6):1069–83. Available from:
657 http://doi.wiley.com/10.1111/mmi.12330
658 20. Brunet YR, Wang X, Rudner DZ. SweC and SweD are essential co-factors of the FtsEX-
659 CwlO cell wall hydrolase complex in *Bacillus subtilis*. PLOS Genet. 2019 Aug
660 22;15(8):e1008296. Available from: https://dx.plos.org/10.1371/journal.pgen.1008296
661 21. Rismondo J, Schulz LM. Not just transporters: Alternative functions of ABC transporters
662 in *Bacillus subtilis* and *Listeria monocytogenes*. Microorganisms. 2021 Jan 13;9(1):163.
663 Available from: https://www.mdpi.com/2076-2607/9/1/163
664 22. Pensinger DA, Gutierrez K V, Smith HB, Vincent WJB, Stevenson DS, Black KA, et al.
665 *Listeria monocytogenes* GlmR is an accessory uridyltransferase essential for cytosolic
666 survival and virulence. bioRxiv. 2021 Jan 1;2021.10.27.466214. Available from:
667 http://biorxiv.org/content/early/2021/10/29/2021.10.27.466214.abstract
668 23. Sun L, Rogiers G, Michiels CW. The natural antimicrobial *trans*-Cinnamaldehyde
669 interferes with UDP-N-acetylglucosamine biosynthesis and cell wall homeostasis in
670 *Listeria monocytogenes*. Foods. 2021 Jul 20;10(7):1666. Available from:
671 https://www.mdpi.com/2304-8158/10/7/1666
672 24. Soldo B, Lazarevic V, Karamata D. *tagO* is involved in the synthesis of all anionic cell-
673 wall polymers in *Bacillus subtilis 168*. Microbiology. 2002 Jul;148(Pt 7):2079–87.
674 25. Watkinson RJ, Hussey H, Baddiley J. Shared lipid phosphate carrier in the biosynthesis
675 of teichoic acid and peptidoglycan. Nat New Biol. 1971 Jan;229(2):57–9.
676 26. Price NPJ, Tsvetanova B. Biosynthesis of the tunicamycins: a review. J Antibiot (Tokyo).
677 2007 Aug;60(8):485–91.
678 27. Campbell J, Singh AK, Santa Maria JP, Kim Y, Brown S, Swoboda JG, et al. Synthetic
679 lethal compound combinations reveal a fundamental connection between wall teichoic
680 acid and peptidoglycan biosyntheses in *Staphylococcus aureus*. ACS Chem Biol. 2011
681 Jan 21;6(1):106–16. Available from: https://pubs.acs.org/doi/10.1021/cb100269f
682 28. Hakulinen JK, Hering J, Brändén G, Chen H, Snijder A, Ek M, et al. MraY-antibiotic
683 complex reveals details of tunicamycin mode of action. Nat Chem Biol. 2017
684 Mar;13(3):265–7.
685 29. Shen Y, Boulos S, Sumrall E, Gerber B, Julian-Rodero A, Eugster MR, et al. Structural
686 and functional diversity in *Listeria* cell wall teichoic acids. J Biol Chem. 2017
687 Oct;292(43):17832–44.
688 30. Brown S, Santa Maria JP, Walker S. Wall teichoic acids of Gram-positive bacteria. Annu
689 Rev Microbiol. 2013 Sep 8;67(1):313–36. Available from:
690 http://www.annualreviews.org/doi/10.1146/annurev-micro-092412-155620
691 31. Vadyvaloo V, Arous S, Gravesen A, Héchard Y, Chauhan-Haubrock R, Hastings JW, et
692 al. Cell-surface alterations in class IIa bacteriocin-resistant *Listeria monocytogenes*

693 strains. Microbiology. 2004 Sep;150(Pt 9):3025–33.
694 32. Boneca IG, Dussurget O, Cabanes D, Nahori M-A, Sousa S, Lecuit M, et al. A critical
695 role for peptidoglycan N-deacetylation in *Listeria* evasion from the host innate immune
696 system. Proc Natl Acad Sci. 2007 Jan 16;104(3):997–1002. Available from:
697 http://www.pnas.org/lookup/doi/10.1073/pnas.0609672104
698 33. Aubry C, Goulard C, Nahori M-A, Cayet N, Decalf J, Sachse M, et al. OatA, a
699 peptidoglycan O-acetyltransferase involved in *Listeria monocytogenes* immune escape,
700 is critical for virulence. J Infect Dis. 2011 Sep 1;204(5):731–40. Available from:
701 https://academic.oup.com/jid/article-lookup/doi/10.1093/infdis/jir396
702 34. Burke TP, Loukitcheva A, Zemansky J, Wheeler R, Boneca IG, Portnoy DA. *Listeria*
703 *monocytogenes* is resistant to lysozyme through the regulation, not the acquisition, of
704 cell wall-modifying enzymes. J Bacteriol. 2014 Nov 1;196(21):3756–67. Available from:
705 https://jb.asm.org/content/196/21/3756
706 35. Durack J, Burke TP, Portnoy DA. A *prl* mutation in SecY suppresses secretion and
707 virulence defects of *Listeria monocytogenes secA2* mutants. J Bacteriol. 2015 Mar
708 1;197(5):932–42. Available from: https://jb.asm.org/content/197/5/932
709 36. Rismondo J, Schulz LM, Yacoub M, Wadhawan A, Hoppert M, Dionne MS, et al. EslB
710 is required for cell wall biosynthesis and modification in *Listeria monocytogenes*. J
711 Bacteriol. 2021 Jan 25;203(4):e00553-20. Available from:
712 http://jb.asm.org/lookup/doi/10.1128/JB.00553-20
713 37. Tesson B, Dajkovic A, Keary R, Marlière C, Dupont-Gillain CC, Carballido-López R.
714 Magnesium rescues the morphology of *Bacillus subtilis mreB* mutants through its
715 inhibitory effect on peptidoglycan hydrolases. Sci Rep. 2022 Jan;12(1):1137.
716 38. Marquardt JL, Brown ED, Lane WS, Haley TM, Ichikawa Y, Wong CH, et al. Kinetics,
717 stoichiometry, and identification of the reactive thiolate in the inactivation of UDP-
718 Glc*N*Ac enolpyruvoyl transferase by the antibiotic fosfomycin. Biochemistry. 1994
719 Sep;33(35):10646–51.
720 39. Howell A, Dubrac S, Andersen KK, Noone D, Fert J, Msadek T, et al. Genes controlled
721 by the essential YycG/YycF two-component system of *Bacillus subtilis* revealed through
722 a novel hybrid regulator approach. Mol Microbiol. 2003 Sep;49(6):1639–55.
723 40. Wamp S, Rutter ZJ, Rismondo J, Jennings CE, Möller L, Lewis RJ, et al. PrkA controls
724 peptidoglycan biosynthesis through the essential phosphorylation of ReoM. Elife. 2020
725 May 29;9:e56048. Available from: https://elifesciences.org/articles/56048
726 41. Wamp S, Rothe P, Stern D, Holland G, Döhling J, Halbedel S. MurA escape mutations
727 uncouple peptidoglycan biosynthesis from PrkA signaling. PLoS Pathog. 2022
728 Mar;18(3):e1010406.
729 42. Du W, Brown JR, Sylvester DR, Huang J, Chalker AF, So CY, et al. Two active forms

730 of UDP-N-acetylglucosamine enolpyruvyl transferase in gram-positive bacteria. J
731 Bacteriol. 2000 Aug;182(15):4146–52.
732 43. Kock H, Gerth U, Hecker M. MurAA, catalysing the first committed step in peptidoglycan
733 biosynthesis, is a target of Clp-dependent proteolysis in *Bacillus subtilis*. Mol Microbiol.
734 2004 Feb;51(4):1087–102.
735 44. Rismondo J, Bender JK, Halbedel S. Suppressor mutations linking *gpsB* with the first
736 committed step of peptidoglycan biosynthesis in *Listeria monocytogenes*. J Bacteriol.
737 2016 Jan 1;199(1):e00393-16. Available from:
738 https://jb.asm.org/lookup/doi/10.1128/JB.00393-16
739 45. Meeske AJ, Riley EP, Robins WP, Uehara T, Mekalanos JJ, Kahne D, et al. SEDS
740 proteins are a widespread family of bacterial cell wall polymerases. Nature. 2016
741 Sep;537(7622):634–8.
742 46. Emami K, Guyet A, Kawai Y, Devi J, Wu LJ, Allenby N, et al. RodA as the missing
743 glycosyltransferase in *Bacillus subtilis* and antibiotic discovery for the peptidoglycan
744 polymerase pathway. Nat Microbiol. 2017 Jan;2:16253.
745 47. Korsak D, Markiewicz Z, Gutkind GO, Ayala JA. Identification of the full set of *Listeria*
746 *monocytogenes* penicillin-binding proteins and characterization of PBPD2 (Lmo2812).
747 BMC Microbiol. 2010 Sep;10:239.
748 48. Rismondo J, Möller L, Aldridge C, Gray J, Vollmer W, Halbedel S. Discrete and
749 overlapping functions of peptidoglycan synthases in growth, cell division and virulence
750 of *Listeria monocytogenes*. Mol Microbiol. 2015 Jan;95(2):332–51. Available from:
751 http://doi.wiley.com/10.1111/mmi.12873
752 49. Huber G, Nesemann G. Moenomycin, an inhibitor of cell wall synthesis. Biochem
753 Biophys Res Commun. 1968 Jan;30(1):7–13.
754 50. Dobihal GS, Brunet YR, Flores-Kim J, Rudner DZ. Homeostatic control of cell wall
755 hydrolysis by the WalRK two-component signaling pathway in *Bacillus subtilis*. Elife.
756 2019 Dec 6;8:e52088. Available from: https://elifesciences.org/articles/52088
757 51. Domínguez□Cuevas P, Porcelli I, Daniel RA, Errington J. Differentiated roles for MreB□
758 actin isologues and autolytic enzymes in *Bacillus subtilis* morphogenesis. Mol Microbiol.
759 2013 Sep 4;89(6):1084–98. Available from:
760 https://onlinelibrary.wiley.com/doi/10.1111/mmi.12335
761 52. Perego M, Glaser P, Minutello A, Strauch MA, Leopold K, Fischer W. Incorporation of
762 D-alanine into lipoteichoic acid and wall teichoic acid in *Bacillus subtilis*. Identification of
763 genes and regulation. J Biol Chem. 1995 Jun;270(26):15598–606.
764 53. Neuhaus FC, Baddiley J. A continuum of anionic charge: structures and functions of D-
765 alanyl-teichoic acids in Gram-positive bacteria. Microbiol Mol Biol Rev. 2003
766 Dec;67(4):686–723.

767 54. Rismondo J, Gillis A, Gründling A. Modifications of cell wall polymers in Gram-positive
768 bacteria by multi-component transmembrane glycosylation systems. Curr Opin
769 Microbiol. 2021 Apr;60:24–33. Available from:
770 https://linkinghub.elsevier.com/retrieve/pii/S1369527421000138
771 55. Peschel A, Otto M, Jack RW, Kalbacher H, Jung G, Götz F. Inactivation of the *dlt* operon
772 in *Staphylococcus aureus* confers sensitivity to defensins, protegrins, and other
773 antimicrobial peptides. J Biol Chem. 1999 Mar 26;274(13):8405–10. Available from:
774 http://www.jbc.org/lookup/doi/10.1074/jbc.274.13.8405
775 56. Wecke J, Madela K, Fischer W. The absence of D-alanine from lipoteichoic acid and
776 wall teichoic acid alters surface charge, enhances autolysis and increases susceptibility
777 to methicillin in *Bacillus subtilis*. Microbiology. 1997 Sep;143(9):2953–60.
778 57. Carroll SA, Hain T, Technow U, Darji A, Pashalidis P, Joseph SW, et al. Identification
779 and characterization of a peptidoglycan hydrolase, MurA, of *Listeria monocytogenes* , a
780 muramidase needed for cell separation. J Bacteriol. 2003 Dec 1;185(23):6801–8.
781 Available from: https://doi.org/10.1128/JB.185.23.6801-6808.2003
782 58. Pilgrim S, Kolb-Mäurer A, Gentschev I, Goebel W, Kuhn M. Deletion of the gene
783 encoding *p60* in *Listeria monocytogenes* leads to abnormal cell division and loss of
784 actin-based motility. Infect Immun. 2003 Jun;71(6):3473–84.
785 59. Eugster MR, Morax LS, Hüls VJ, Huwiler SG, Leclercq A, Lecuit M, et al. Bacteriophage
786 predation promotes serovar diversification in *Listeria monocytogenes*. Mol Microbiol.
787 2015 Jul;97(1):33–46.
788 60. Rismondo J, Percy MG, Gründling A. Discovery of genes required for lipoteichoic acid
789 glycosylation predicts two distinct mechanisms for wall teichoic acid glycosylation. J Biol
790 Chem. 2018 Mar 2;293(9):3293–306. Available from:
791 http://www.jbc.org/lookup/doi/10.1074/jbc.RA117.001614
792 61. Sassine J, Sousa J, Lalk M, Daniel RA, Vollmer W. Cell morphology maintenance in
793 *Bacillus subtilis* through balanced peptidoglycan synthesis and hydrolysis. Sci Rep.
794 2020;10(1):17910. Available from: https://doi.org/10.1038/s41598-020-74609-5
795 62. Lai GC, Cho H, Bernhardt TG. The mecillinam resistome reveals a role for peptidoglycan
796 endopeptidases in stimulating cell wall synthesis in *Escherichia coli*. PLoS Genet. 2017
797 Jul;13(7):e1006934.
798 63. Van Heijenoort Y, Derrien M, Van Heijenoort J. Polymerization by transglycosylation in
799 the biosynthesis of the peptidoglycan of *Escherichia coli* K 12 and its inhibition by
800 antibiotics. FEBS Lett. 1978 May;89(1):141–4.
801 64. Ostash B, Walker S. Moenomycin family antibiotics: chemical synthesis, biosynthesis,
802 and biological activity. Nat Prod Rep. 2010 Nov;27(11):1594–617.
803 65. Percy MG, Gründling A. Lipoteichoic acid synthesis and function in Gram-positive

804 bacteria. Annu Rev Microbiol. 2014 Sep 8;68(1):81–100. Available from:
805 https://doi.org/10.1146/annurev-micro-091213-112949
806 66. Herbert S, Bera A, Nerz C, Kraus D, Peschel A, Goerke C, et al. Molecular basis of
807 resistance to muramidase and cationic antimicrobial peptide activity of lysozyme in
808 staphylococci. PLoS Pathog. 2007 Jul;3(7):e102.
809 67. Steudle A, Pleiss J. Modelling of lysozyme binding to a cation exchange surface at
810 atomic detail: the role of flexibility. Biophys J. 2011 Jun;100(12):3016–24.
811 68. Low LY, Yang C, Perego M, Osterman A, Liddington R. Role of net charge on catalytic
812 domain and influence of cell wall binding domain on bactericidal activity, specificity, and
813 host range of phage lysins. J Biol Chem. 2011 Sep;286(39):34391–403.
814 69. Weidenmaier C, Kristian SA, Peschel A. Bacterial resistance to antimicrobial host
815 defenses--an emerging target for novel antiinfective strategies? Curr Drug Targets.
816 2003 Nov;4(8):643–9.
817 70. Ragland SA, Criss AK. From bacterial killing to immune modulation: Recent insights into
818 the functions of lysozyme. PLoS Pathog. 2017 Sep;13(9):e1006512.
819 71. Delaune A, Poupel O, Mallet A, Coic Y-M, Msadek T, Dubrac S. Peptidoglycan
820 crosslinking relaxation plays an important role in *Staphylococcus aureus* WalKR-
821 dependent cell viability. PLoS One. 2011 Feb 28;6(2):e17054. Available from:
822 https://dx.plos.org/10.1371/journal.pone.0017054
823 72. Delauné A, Dubrac S, Blanchet C, Poupel O, Mäder U, Hiron A, et al. The WalKR system
824 controls major staphylococcal virulence genes and is involved in triggering the host
825 inflammatory response. Infect Immun. 2012 Oct;80(10):3438–53.
826 73. Dubrac S, Msadek T. Identification of genes controlled by the essential YycG/YycF two-
827 component system of *Staphylococcus aureus*. J Bacteriol. 2004 Feb 15;186(4):1175–
828 81. Available from: https://jb.asm.org/content/186/4/1175
829 74. Fischer M, Engelgeh T, Rothe P, Fuchs S, Thürmer A, Halbedel S. *Listeria*
830 *monocytogenes* gene essentiality under laboratory conditions and during macrophage
831 infection. bioRxiv. 2022 Jan 1;2022.03.04.482958. Available from:
832 http://biorxiv.org/content/early/2022/03/04/2022.03.04.482958.abstract
833 75. Salamaga B, Kong L, Pasquina-Lemonche L, Lafage L, von und zur Muhlen M, Gibson
834 JF, et al. Demonstration of the role of cell wall homeostasis in *Staphylococcus aureus*
835 growth and the action of bactericidal antibiotics. Proc Natl Acad Sci. 2021 Nov
836 2;118(44):e2106022118. Available from:
837 https://pnas.org/doi/full/10.1073/pnas.2106022118
838 76. Lauer P, Chow MYN, Loessner MJ, Portnoy DA, Calendar R. Construction,
839 characterization, and use of two *Listeria monocytogenes* site-specific phage integration
840 vectors. J Bacteriol. 2002 Aug;184(15):4177–86.

841 77. Camilli A, Tilney LG, Portnoy DA. Dual roles of *plcA* in *Listeria monocytogenes*
842 pathogenesis. Mol Microbiol. 1993 Apr;8(1):143–57. Available from:
843 https://onlinelibrary.wiley.com/doi/10.1111/j.1365-2958.1993.tb01211.x
844 78. Kang J, Wiedmann M, Boor KJ, Bergholz TM. VirR-Mediated resistance of *Listeria*
845 *monocytogenes* against food antimicrobials and cross-protection induced by exposure
846 to organic acid salts. Appl Environ Microbiol. 2015 Jul 1;81(13):4553–62. Available from:
847 http://aem.asm.org/lookup/doi/10.1128/AEM.00648-15
848 79. Miller JH. Experiments in Molecular Genetics. NY: Cold Spring Harbor Laboratory; 1972.
849 352–355 p.
850 80. Pazos M, Peters K. Peptidoglycan. Subcell Biochem. 2019;92:127–68.
851 81. Sarkar P, Yarlagadda V, Ghosh C, Haldar J. A review on cell wall synthesis inhibitors
852 with an emphasis on glycopeptide antibiotics. Medchemcomm. 2017 Mar;8(3):516–33.
853

854 **Figure legends**

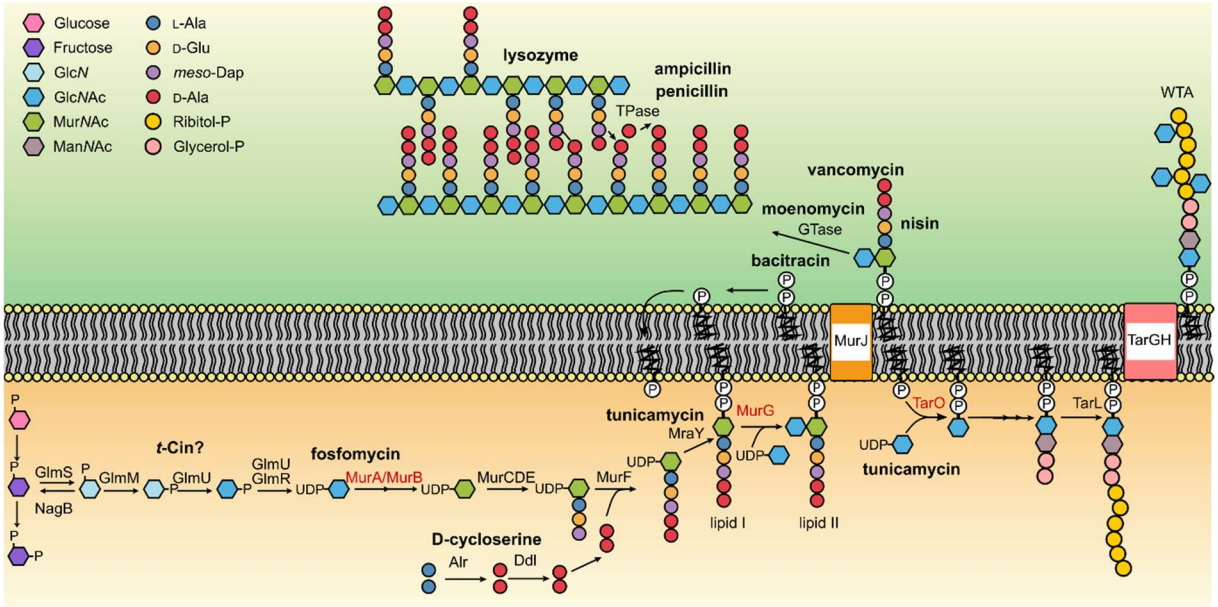

855

856 **Figure 1: Schematic of the UDP-Glc*N*Ac, peptidoglycan and wall teichoic acid**
857 **biosynthesis pathway.** UDP-Glc*N*Ac, which is required for peptidoglycan and wall teichoic
858 acid (WTA) biosynthesis, is synthesized from Fructose-6-phosphate in a four-step reaction
859 catalyzed by GlmS, GlmM, GlmU and GlmR. MurA, an UDP-Glc*N*Ac-1-
860 carboxyvinyltransferase catalyzing the first step of peptidoglycan biosynthesis, and MurB
861 convert UDP-Glc*N*Ac to UDP-Mur*N*Ac. Lipid II is produced in subsequent steps, which are
862 performed by MurCDEF, Alr, Ddl, MraY and MurG, flipped across the membrane by MurJ and
863 inserted into the growing glycan strand by glycosyltransferases (GTases). Finally,
864 peptidoglycan is crosslinked by the action of transpeptidases (TPases) (80). UDP-Glc*N*Ac also
865 serves as a substrate of TarO, the first enzyme of the WTA biosynthesis pathway. After the
866 WTA polymer is synthesized by a subset of enzymes, it is transported across the membrane
867 via TarGH (30) and, in case of *L. monocytogenes* 10403S, decorated with Glc*N*Ac residues
868 (29). UDP-Glc*N*Ac-consuming enzymes are labelled in red. Antibiotics targeting different steps
869 of the UDP-Glc*N*Ac, peptidoglycan and WTA biosynthesis pathways or degrade peptidoglycan
870 are depicted in bold (22,27,81).

871

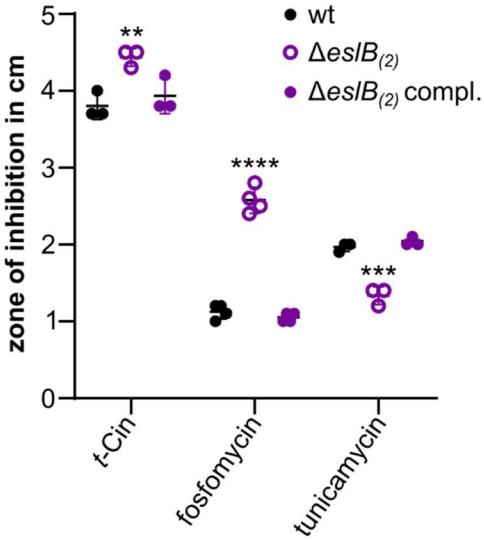

872

873 **Figure 2: Alterations in the resistance of the *eslB* mutant towards cell wall-targeting**
874 **antibiotics.** Disk diffusion assay. *L. monocytogenes* strains 10403S (wt), Δ*eslB*$_{(2)}$ and Δ*eslB*$_{(2)}$
875 compl. were spotted on BHI plates. Antibiotic-soaked disks placed on top the agar surface and
876 the plates incubated for 24h at 37°C. The inhibition zones for the indicated strains were
877 measured and the average values and standard deviation of at least three independent
878 experiments were plotted. For statistical analysis, a one-way ANOVA coupled with a Dunnett's
879 multiple comparison test was used (** $p \leq 0.01$, *** $p \leq 0.001$, **** $p \leq 0.0001$).

880

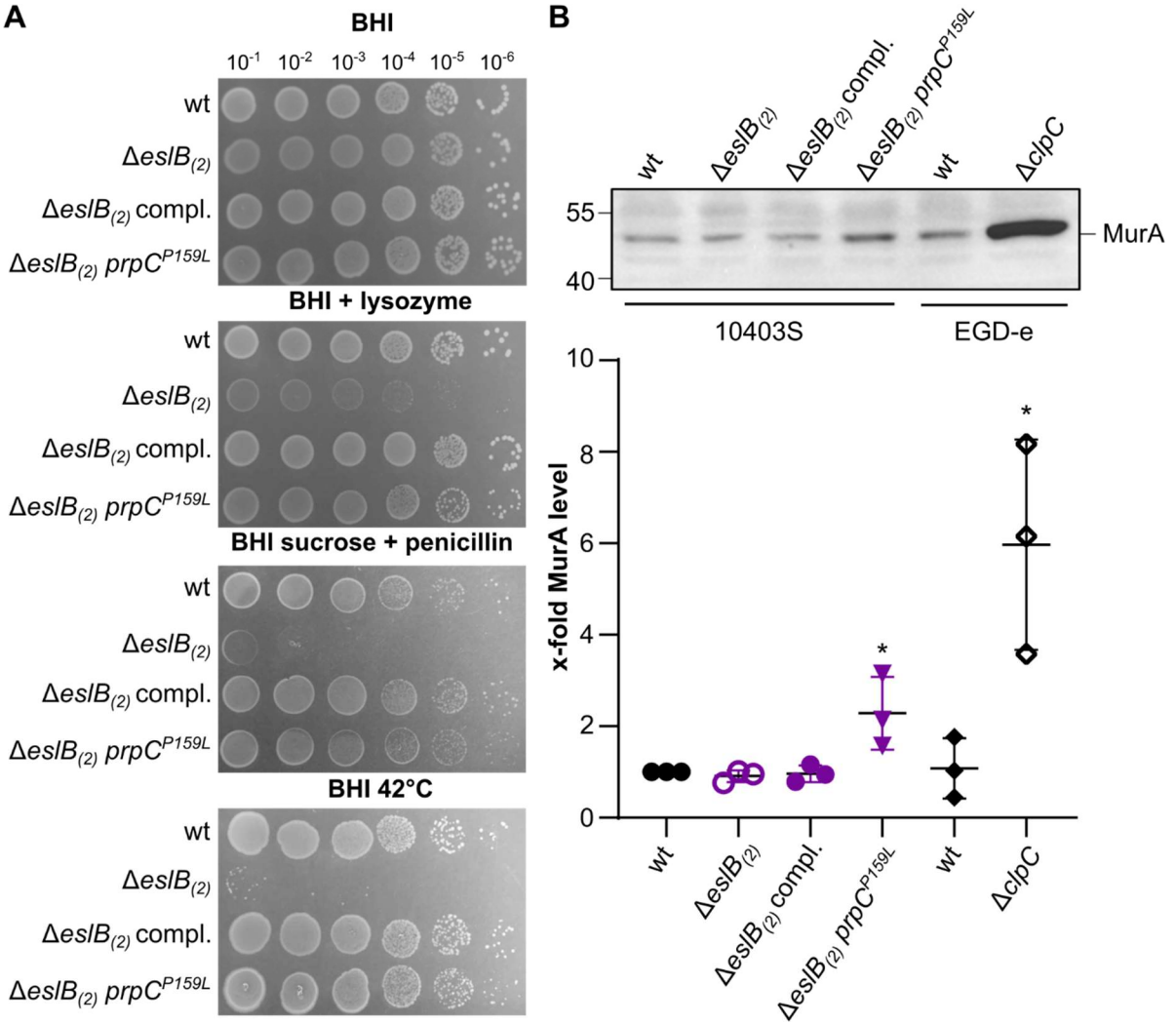

Figure 3: Mutation P159L in *prpC* suppresses *eslB* phenotypes. (A) Drop dilution assay. Dilutions of *L. monocytogenes* strains 10403S (wt), Δ*eslB*$_{(2)}$, Δ*eslB*$_{(2)}$ compl., and Δ*eslB*$_{(2)}$ *prpC*^{P159L} were spotted on BHI plates, BHI plates containing 100 µg/ml lysozyme or containing 0.5 M sucrose and 0.025 µg/ml penicillin G and were incubated at 37°C or on BHI plates and were incubated at 42°C. (B) Western blot. Protein samples of strains 10403S, Δ*eslB*$_{(2)}$, Δ*eslB*$_{(2)}$ compl. and Δ*eslB*$_{(2)}$ *prpC*^{P159L} were separated by SDS PAGE and transferred to a PVDF membrane. MurA was detected using a MurAA-specific antibody as described in the methods section. Protein samples of *L. monocytogenes* wildtype strain EGD-e and a *clpC* mutant were used as controls. MurA level in the protein samples were quantified and plotted. For statistical analysis, an unpaired two-tailed t-test was used (* $p \leq 0.05$).

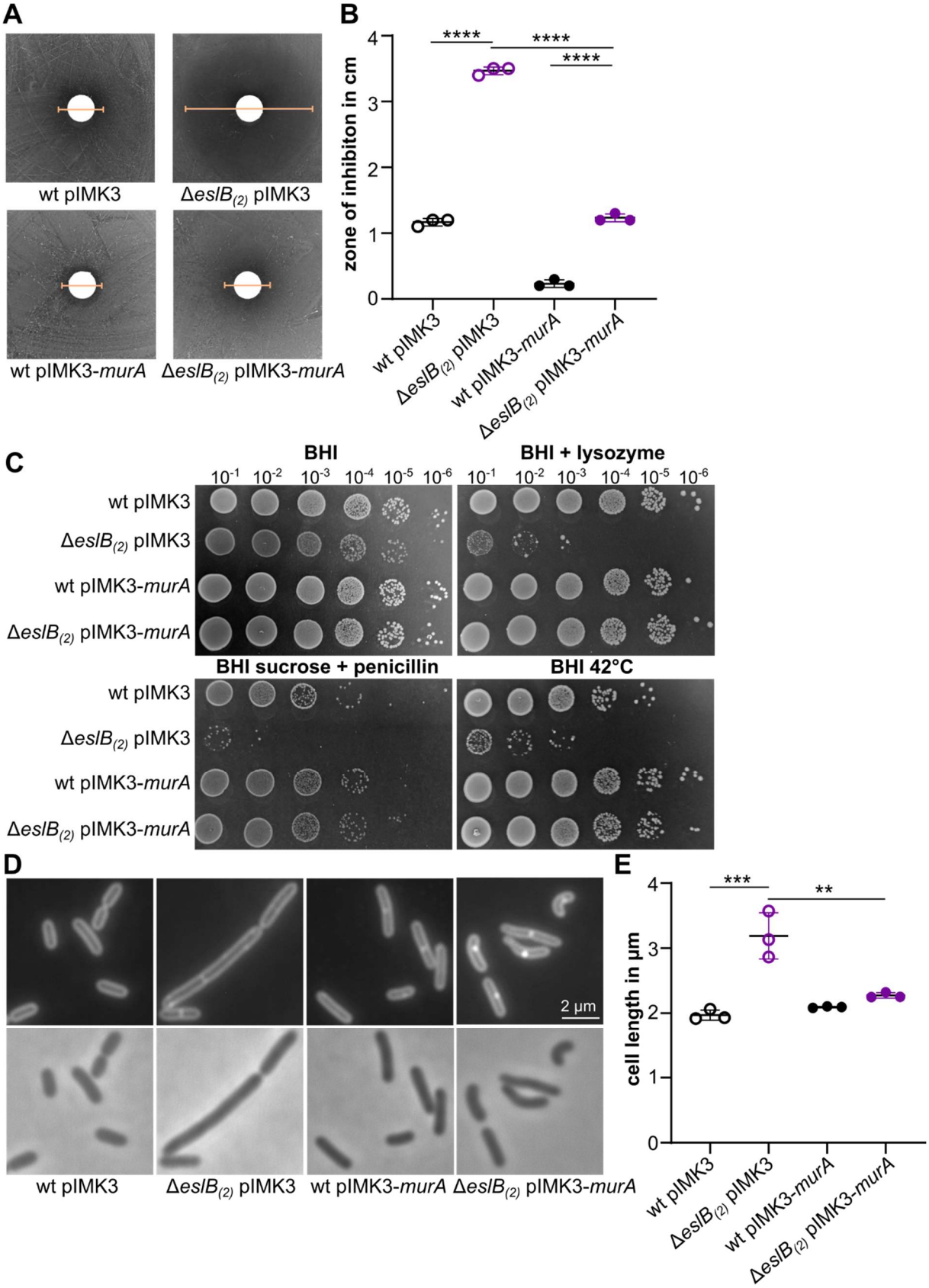

Figure 4: MurA overexpression leads to suppression of *eslB* phenotypes. (A-B) Fosfomycin disk diffusion assay. (A) *L. monocytogenes* strains wt pIMK3, Δ*eslB* pIMK3, wt pIMK3-*murA* and Δ*eslB* pIMK3-*murA* were plated on BHI plates containing 1 mM IPTG.

897 Fosfomycin-soaked disks were placed on the agar surface and the plates incubated for 24 h
898 at 37°C. Yellow lines indicate the diameter of the zone of inhibition. (B) The inhibition zones
899 for the indicated strains were measured and the average values and standard deviation of
900 three independent experiments were plotted. (C) Drop dilution assay. Dilutions of *L.*
901 *monocytogenes* strains 10403S pIMK3 (wt pIMK3), Δ*eslB* pIMK3, wt pIMK3-*murA* and Δ*eslB*
902 pIMK3-*murA* were spotted on BHI plates, BHI plates containing 100 µg/ml lysozyme or
903 containing 0.5 M sucrose and 0.025 µg/ml penicillin G, which were incubated at 37°C or on
904 BHI plates, which were incubated at 42°C. (D) Microscopy images of *L. monocytogenes*
905 strains. Bacterial membranes were stained with nile red as described in the methods section.
906 Scale bar is 2 µm. (E) Cell length of *L. monocytogenes* strains shown in panel B. The cell
907 length of 50 cells per strain was determined and the median cell length calculated. The average
908 values and standard deviations of three independent experiments are plotted. For statistical
909 analysis, a one-way ANOVA coupled with Tukey‘s multiple comparison test was used (** $p \leq$
910 0.01, *** $p \leq 0.001$, **** $p \leq 0.0001$).

911

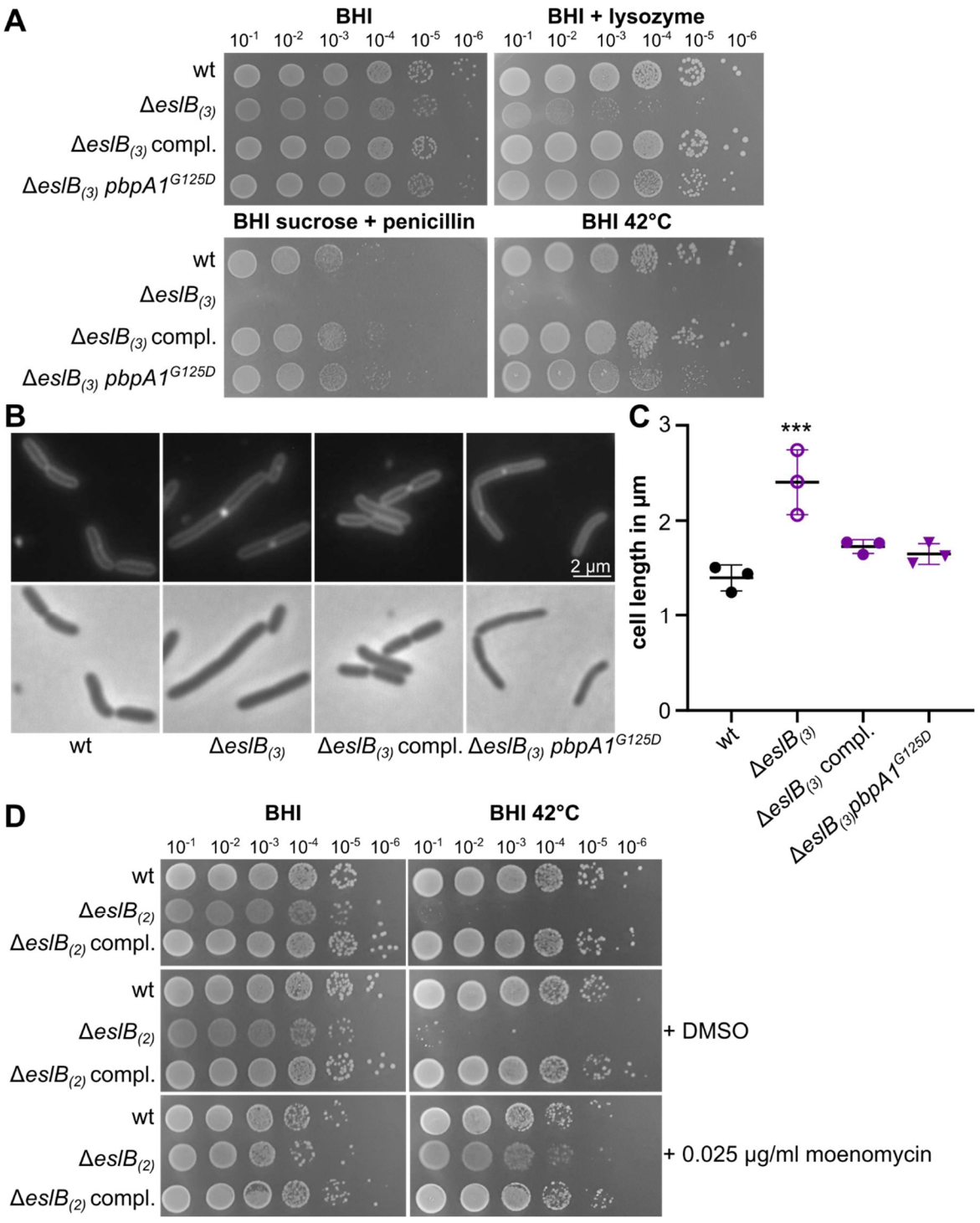

Figure 5: Inactivation of the glycosyltransferase of penicillin binding proteins rescues the *eslB* mutant. (A) Drop dilution assay. Dilutions of *L. monocytogenes* strains 10403S (wt), Δ*eslB*$_{(3)}$, Δ*eslB*$_{(3)}$ compl. and Δ*eslB*$_{(3)}$ *pbpA1*^{G125D} were spotted on BHI plates, BHI plates containing 100 µg/ml lysozyme or containing 0.5 M sucrose and 0.025 µg/ml penicillin G, which were incubated at 37°C or on BHI plates, which were incubated at 42°C. (B) Microscopy images of *L. monocytogenes* strains. Bacterial membranes were stained with nile red as described in the methods section. Scale bar is 2 µm. (C) Cell length of *L. monocytogenes* strains shown in panel B. The cell length of 50 cells per strain was determined and the median

921 cell length calculated. The average values and standard deviations of three independent
922 experiments are plotted. (D) Drop dilution assay. Dilutions of *L. monocytogenes* strains
923 10403S (wt), Δ*eslB*$_{(2)}$ and Δ*eslB*$_{(2)}$ compl. were spotted on BHI plates, BHI plates containing
924 DMSO or containing 0.025 µg/ml moenomycin and incubated at 37°C or 42°C.

925

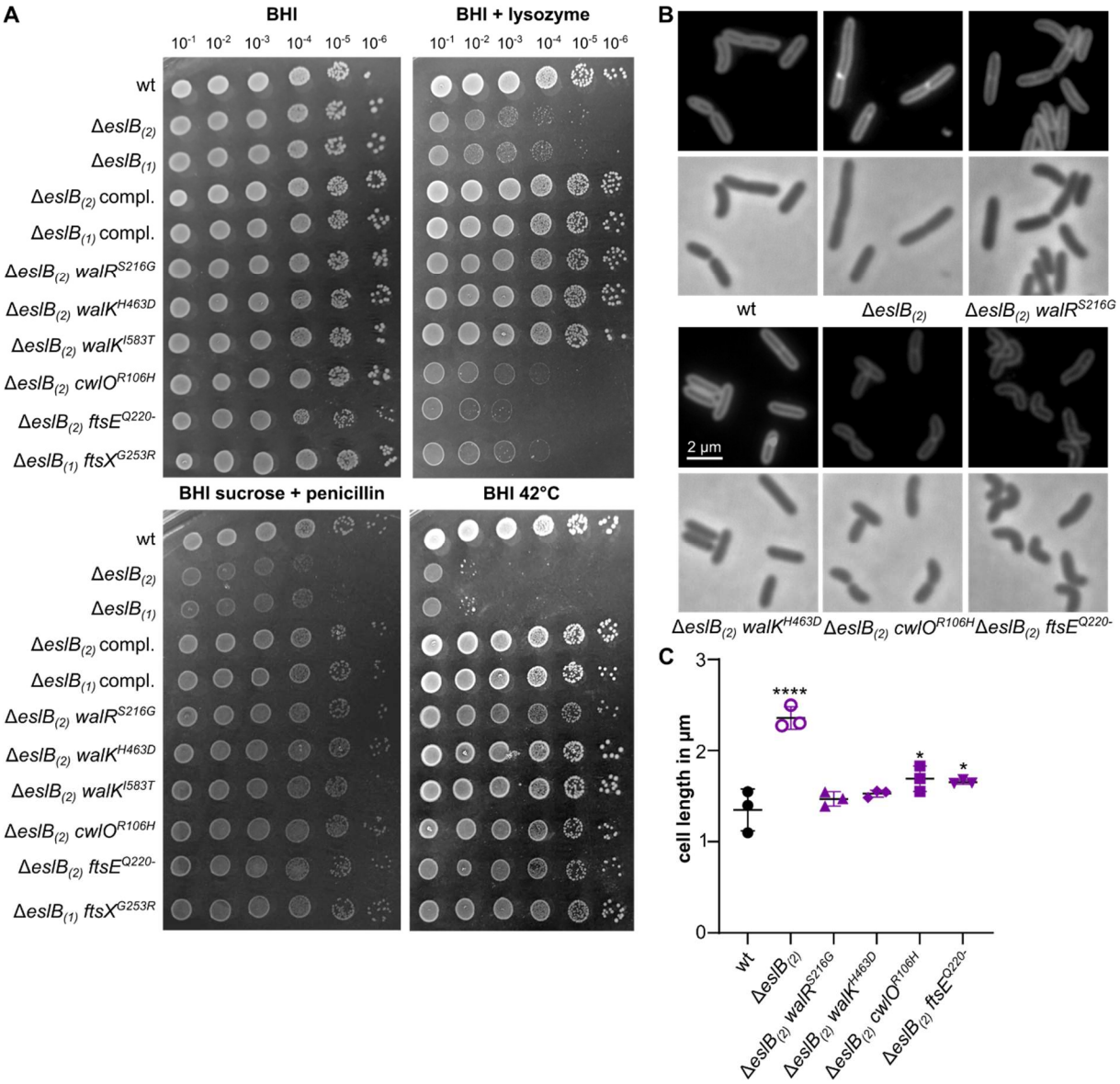

926

927 **Figure 6: Mutations in *walR, walK, cwlO, ftsE* and *ftsX* suppress *eslB* phenotypes.** (A)
928 Drop dilution assay. Dilutions of *L. monocytogenes* strains 10403S (wt), Δ*eslB*$_{(2)}$, Δ*eslB*$_{(1)}$,
929 Δ*eslB*$_{(2)}$ compl., Δ*eslB*$_{(1)}$ compl., Δ*eslB*$_{(2)}$ *walR*^{S216G}, Δ*eslB*$_{(2)}$ *walK*^{H463D}, Δ*eslB*$_{(2)}$ *walK*^{I583T},
930 Δ*eslB*$_{(2)}$ *cwlO*^{R106H}, Δ*eslB*$_{(2)}$ *ftsE*$^{Q220-}$ and Δ*eslB*$_{(1)}$ *ftsX*^{G253R} were spotted on BHI plates, BHI
931 plates containing 100 µg/ml lysozyme or containing 0.5 M sucrose and 0.025 µg/ml penicillin
932 G and were incubated at 37°C or on BHI plates that were incubated at 42°C. (B) Microscopy
933 images of *L. monocytogenes* strains. Bacterial membranes were stained with nile red as
934 described in the methods section. Scale bar is 2 µm. (C) Cell length of *L. monocytogenes*

935 strains shown in panel B. The cell length of 50 cells per strain was determined and the median
936 cell length calculated. The average values and standard deviations of three independent
937 experiments are plotted. For statistical analysis, a one-way ANOVA coupled with a Dunnett's
938 multiple comparison test was used (* $p \leq 0.05$, **** $p \leq 0.0001$).

939

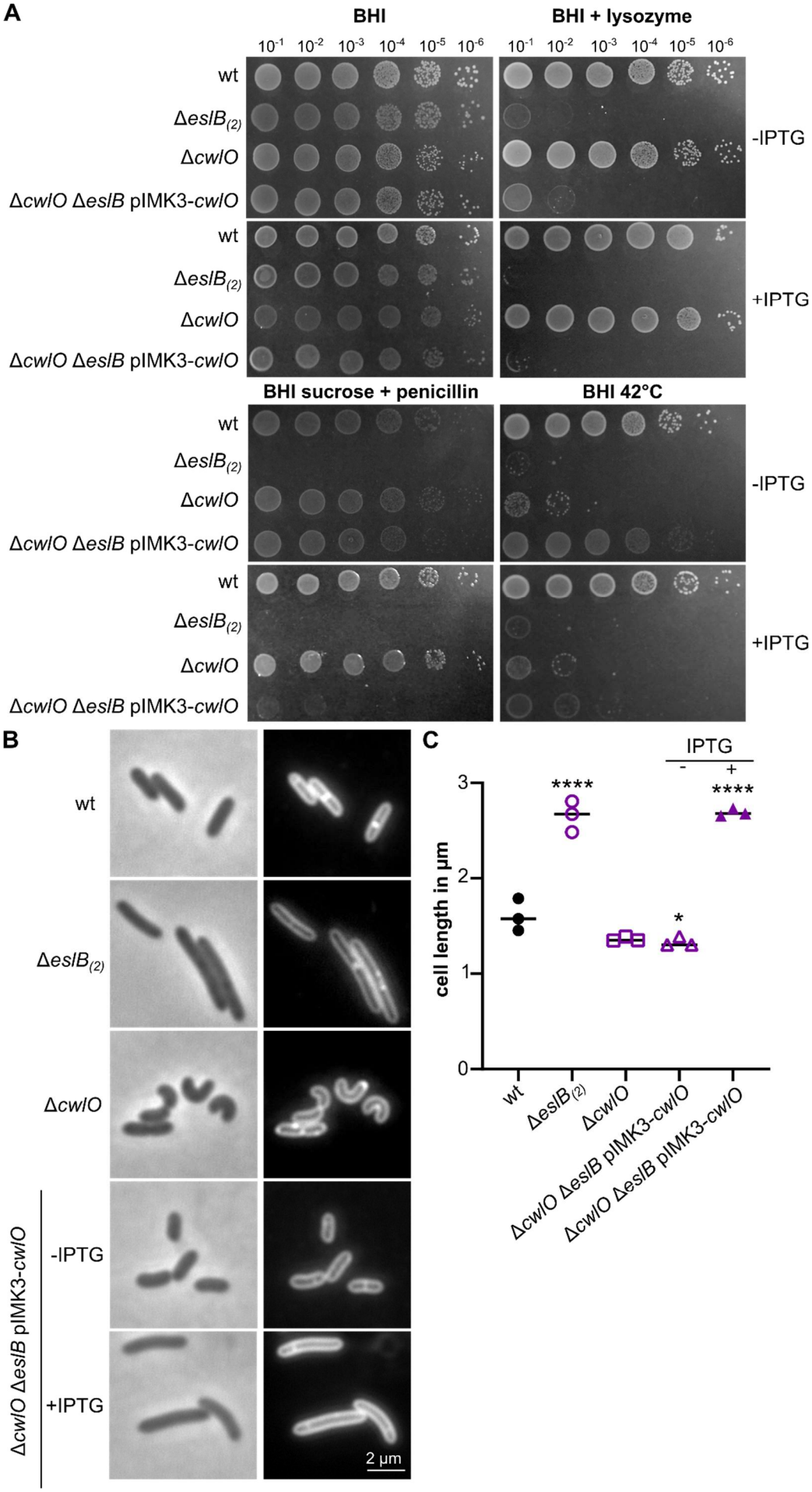
A
BHI
BHI + lysozyme
10-1 10-2 10-3 10-4 10-5 10-6
wt
ΔeslB(2)
ΔcwlO
ΔcwlO ΔeslB pIMK3-cwlO
-IPTG
+IPTG
BHI sucrose + penicillin
BHI 42°C
B
wt
ΔeslB(2)
ΔcwlO
ΔcwlO ΔeslB pIMK3-cwlO
-IPTG
+IPTG
2 µm
C
IPTG
-
+
cell length in µm
0
1
2
3
****
*
wt
ΔeslB(2)
ΔcwlO
ΔcwlO ΔeslB pIMK3-cwlO
ΔcwlO ΔeslB pIMK3-cwlO

940

941 **Figure 7: Absence of CwlO suppresses most of the *eslB* phenotypes.** (A) Drop dilution
942 assay. Dilutions of *L. monocytogenes* strains 10403S (wt), Δ*eslB*$_{(2)}$, Δ*cwlO* and Δ*cwlO* Δ*eslB*
943 pIMK3-*cwlO* were spotted on BHI plates, BHI plates containing 100 µg/ml lysozyme or
944 containing 0.5 M sucrose and 0.025 µg/ml penicillin G and were incubated at 37°C or on BHI
945 plates that were incubated at 42°C. For induction of *cwlO* expression, the indicated plates were
946 supplemented with 1 mM IPTG. (B) Microscopy images of *L. monocytogenes* strains. Bacterial
947 membranes were stained with nile red as described in the methods section. Scale bar is 2 µm.
948 (C) Cell length of *L. monocytogenes* strains shown in panel B. The cell length of 50 cells per
949 strain was determined and the median cell length calculated. The average values and standard
950 deviations of three independent experiments are plotted. For statistical analysis, a one-way
951 ANOVA coupled with a Dunnett's multiple comparison test was used (* $p \leq 0.05$, **** $p \leq$
952 0.0001).

953

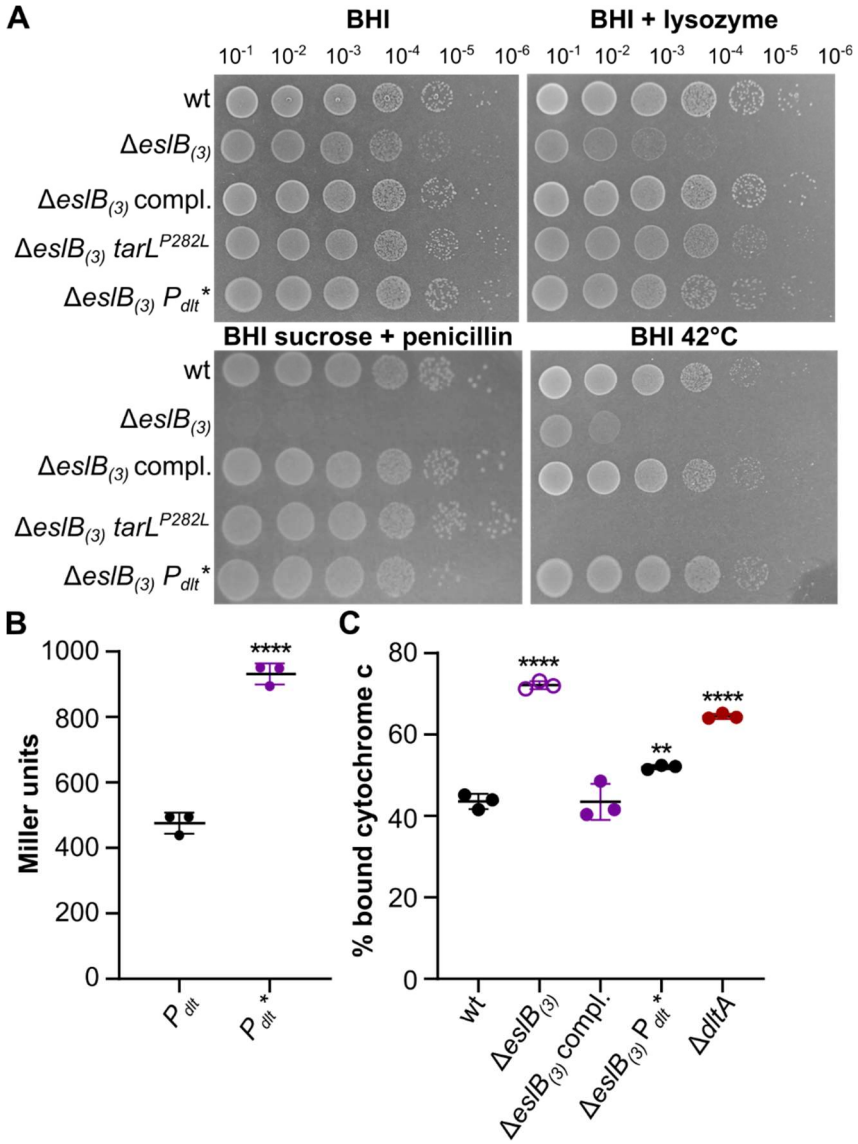

954

955 **Figure 8: Suppression of *eslB* phenotypes by alterations in WTA biosynthesis and**
956 **modification.** (A) Drop dilution assay. Dilutions of *L. monocytogenes* strains 10403S (wt),
957 Δ*eslB*$_{(3)}$, Δ*eslB*$_{(3)}$ compl., Δ*eslB*$_{(3)}$ *tarL*^{P282L} and Δ*eslB*$_{(3)}$ P_{dlt}^{*} were spotted on BHI plates, BHI
958 plates containing 100 µg/ml lysozyme or containing 0.5 M sucrose and 0.025 µg/ml penicillin
959 G and were incubated at 37°C or on BHI plates that were incubated at 42°C. (B) β-
960 galactosidase assay. The *dlt* promoter of *L. monocytogenes* wildtype 10403S (P_{dlt}) and
961 suppressor strain Δ*eslB*$_{(3)}$ P_{dlt}^{*} (P_{dlt}^{*}) were fused with *lacZ* and integrated into the *amyE* locus
962 of *Bacillus subtilis*. The promoter activity was determined in Miller units as described in the
963 methods section and the average and standard deviation of three independent experiments
964 were plotted. An unpaired t-test was used for statistical analysis (**** $p \leq 0.0001$). (C)
965 Cytochrome C assay. Cells *of L. monocytogenes* strains 10403S, Δ*eslB*$_{(3)}$, Δ*eslB*$_{(3)}$ compl. and
966 Δ*eslB*$_{(3)}$ P_{dlt}^{*} were incubated with cytochrome C as described in the methods section. The
967 percentage of cytochrome C, which is bound by the cell surface, was calculated for three
968 independent experiments and plotted. A strain lacking DltA was used as control. For statistical
969 analysis, a one-way ANOVA coupled with a Dunnett's multiple comparison test was used (** p
970 ≤ 0.01, **** $p \leq 0.0001$).

971

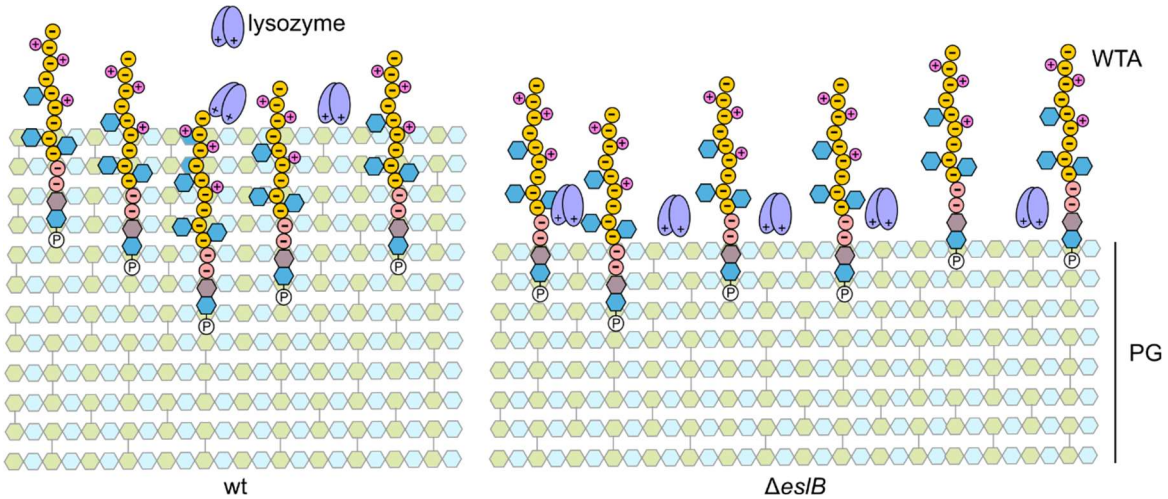

972

973 **Figure 9: Model of altered WTA presentation on the cell surface of an *eslB* mutant.** The
974 Gram-positive cell wall is composed of a thick layer of peptidoglycan (PG) and wall teichoic
975 acids (WTA), which are attached to the Mur*N*Ac-moiety of the PG backbone (30). WTA of *L.*
976 *monocytogenes* 10403S are composed of a negatively charged ribitol phosphate backbone
977 (indicated by -), which can be modified with Glc*N*Ac residues (blue hexagons) and positively
978 charged D-alanine residues (indicated by +). The absence of EslB seems to affect the
979 production and/or distribution of the PG precursor UDP-Glc*N*Ac between different pathways,
980 which results in the production of a thinner PG layer. WTAs are thought to partially stick out of
981 the PG layer and we propose that due to the thinner PG layer produced by the *eslB* mutant, a

982 larger portion of the WTA backbone, which is negatively charged, could be presented on the
983 bacterial cell surface. This would result in a higher negative cell surface charge of the *eslB*
984 mutant, which would affect the binding capability and/or activity of PG hydrolases, lysozyme
985 and cationic antimicrobial peptides (67–70).

986

987